Winter 1997

An Investigation on the Effect of Aging and Fatigue Damage on the Mechanical Properties of a Graphite/Bismaleimide Composite

William M. Johnston Jr.
Old Dominion University

AN INVESTIGATION ON THE EFFECT OF AGING AND FATIGUE DAMAGE ON THE MECHANICAL PROPERTIES OF A GRAPHITE/BISMALEIMIDE COMPOSITE

by

William M. Johnston Jr.
B. S. June 1993, Old Dominion University

A Thesis submitted to the Faculty of
Old Dominion University in Partial Fulfillment of the
Requirement for the Degree of

MASTER OF SCIENCE
ENGINEERING MECHANICS

OLD DOMINION UNIVERSITY
December 1997

Approved by:

R. Prabhakaran (Co-Chair)

Y. Mikata (Co-Chair)

T. S. Gates (Member)

K. Williamson (Member)

ABSTRACT

AN INVESTIGATION ON THE EFFECT OF AGING AND FATIGUE DAMAGE ON THE MECHANICAL PROPERTIES OF A GRAPHITE/BISMALEIMIDE COMPOSITE

William M. Johnston Jr.
Old Dominion University, 1997
Director: T. Gates

This investigation utilizes the open hole tension (OHT) specimen loaded in tension-tension fatigue under isothermal, fixed frequency conditions. A range of load levels and temperature levels where chosen to assess performance. These loads and temperatures ranged from relatively benign conditions (low stress, room temperature) up through aggressive conditions (high stress, high temperature). Measurements of stiffness, damage accumulation, residual strength, weight loss, and glass transition temperature (Tg) were made. Results from this work will help explain the roles of aging, load and fatigue in the performance of elevated temperature OHT specimens as well as provide insights to the individual and synergistic contributions of each process.

Co-Chairs of Thesis Committee: Dr. R. Prabhakaran
Dr. Y. Mikata

TABLE OF CONTENTS

LIST OF TABLES

LIST OF FIGURES

CHAPTER I

INTRODUCTION

New polymer matrix composites (PMCs) are being developed for high temperature applications in both civilian and military aerospace vehicles. The issue of long term durability at elevated temperature is crucial for material selection for these critical structural applications. To address the problems presented by these new materials at elevated temperature, accelerated test methods and associated life prediction models must be developed that provide the means for predicting long term behavior from short term test data. Before these predictive models and accelerated test methods can be developed, a basic understanding of the effects of elevated temperatures and varied load histories on a PMC's mechanical properties is needed.

Predicting the response of a composite laminate to fatigue loading requires an understanding of the basic processes that change the mechanical performance of the material. Once these processes are identified they can be accounted for in modeling. Many attempts have been made to model fatigue in PMCs which have varied from empirical relationships to mechanics based models[1-7].

Mechanics based modeling has the ability to account for much more complicated material responses than empirical models. Some of the more comprehensive models include the continuum damage mechanics models introduced by Harris, Allen and Coats[1-5] and Talreja [6 ,7]. These models use representative volumes to model PMCs. The volume element's stiffness is computed from

constituent mechanical properties and a collection of internal state variables that represent damage. The accumulated damage is averaged over representative volumes and then related to properties such as strength and stiffness. The internal state variables are dependent on the damage propagation laws for the different damage modes (e.g. matrix cracking and delamination).

Most of these models have not been applied to elevated temperature situations. As temperatures increase, the process of aging will play a more critical role in the fatigue performance of PMCs. It is important to understand the interactions of the processes of aging and damage accumulation so they can be modeled. The research herein contributes to this understanding.

Motivation and Objective

Three potential processes contribute to degradation of mechanical performance during a fatigue/aging study. These processes are: chemical aging, physical aging, and damage development [8, 9, 10] Physical aging is a thermo-reversible process believed to depend on the free volume evolution of the polymer, whereas chemical aging is a thermo-irreversible process caused by continued crosslinking in the matrix and oxidative breakdown [8]. Both types of aging are temperature dependent. In general, chemical aging and physical aging are processes that cause the polymer matrix to become stiffer and more brittle, and cause the creep and the stress relaxation rates to be reduced[8]. The damage accumulation during fatigue is a process that will cause the laminate stiffness and strength to decrease due to cracking[7].

These processes are not independent and can be additive or subtractive depending on the test material and the resultant performance property being considered. The continuation of the crosslinking reaction portion of chemical aging results in continued cure in the matrix. Mechanical performance of composite materials have been shown to be dependent on the extent of cure[11-14]. The resulting changes in the matrix materials mechanical properties cause changes in the accumulation and extent of damage. Damage in turn increases the rate of chemical change by increasing the reactive surface area available for oxidative breakdown. Therefore, to correctly model long term elevated temperature behavior of such PMCs from short term testing, the individual effects and interactions of aging and damage accumulation must be accounted for.

The objective of this research was to determine the effects of elevated temperature and fatigue loading on a graphite/bismaleimide composite. A fatigue and aging study was performed on a graphite/bismaleimide (GR/BMI) composite. Testing was designed to determine the individual and synergistic combinations of responses caused by the loading and the elevated temperature. These responses were then related to physical processes known to cause changes in the mechanical performance of PMCs. The effect of the temperature and fatigue loading on the PMCs were quantified by measurements of stiffness, glass transition temperature (Tg), weight loss, fatigue damage, and residual strength.

Overview

The remaining chapters of the text are constructed as follows. Chapter two contains background information. The composite material used is discussed. Information on the chemical aging of fatigue damage of polymer matrix composites is given. Fatigue of composites, damage propagation and damage development are discussed. Chapter three explains the experimental program. Experimental methods and equipment used for the fatigue and aging work are discussed. Specimen preparations and diagrams of the specimens used are presented. Next, this chapter covers initial testing and setup. Equipment alignment and calibration are considered. All testing procedures, data reduction and analysis techniques are explained. Chapter four presents the experimental results of fatigue and isothermal aging investigations. Presentation order is developed so conclusions can be drawn in a logical manner. Chapter five starts with a discussion of all results and their relation to each other and ends with conclusions.

The effects of temperature and loading during fatigue on the mechanical properties are explained. The implications and connections to the processes of aging and damage accumulations are discussed. Final conclusions are also drawn to develop an understanding of fatigue damage and aging that occurred during this elevated temperature fatigue.

CHAPTER II

BACKGROUND

Although polymer matrix composites have many advantages for use in critical components on aero-structures, certain properties related to damage tolerance, damage resistance, and unknown long term durability play a critical role in limiting their application. Both processes of aging and fatigue damage accumulation play roles in determining the long term performance of a PMC.

Material Information

Material system

Tests were performed on a G40-800/5260 composite material system. This system consisted of a high strength, intermediate modulus carbon fiber produced by Celion in a toughened bismaleimide (BMI) matrix that was produced by BASF. Test panels were produced at NASA Langley Research Center with a $[45,0,-45,90]_{2S}$ quasi-isotropic lay-up and a nominal thickness of 2.16 mm (0.085 in) after cure.

Cure Cycle

The panels were cured using the manufacturer's recommended procedure. A two step cure cycle was used. The temperature was raised from room temperature to 149°C at 1.6°C/min. and held for thirty minutes under vacuum. After this first stage the pressure was increased to 586 kPa (85 psi.) in the autoclave and the temperature was raised to 191°C at 1.6°C/min. These conditions were maintained for four hours. Finally, the specimens were cooled to room temperature and pressure was released.

Interleaving

Delamination failures, where the laminate disbonds or cracks occur between laminae, can initiate from small impact areas[15, 16, 17] fatigue[7, 18-25], edge effects[26], holes[26-30], manufacturing defects[15], environmental effects [31, 32], and synergistic combinations of any of these factors. These problems have led to the development of a technique know as interleaving.

The concept of interleaving is simple; it only requires the introduction of an advantageous (tough) material between laminates. The purpose of this layer is twofold. First, the presence of the inter laminar layer reduces the magnitude of the inter-laminar stresses, and may locally strengthen the ply interface. Second, if delamination does occur the tough layer requires more energy than a conventional laminate to propagate the damage[33]. Attainment of delamination resistance and requirements for higher use temperatures has lead to interleave toughened matrix materials such as 5260.

The addition of an interleave complicates the process of modeling. Interleaves add another phase of material to the matrix increasing the complexity required to predict the response of the final material accurately. Aging models need to contend with multiple chemically distinct materials with distinct responses to time at elevated temperature.

Chemical Aging Process

Two significant mechanisms contribute to the degradation of the mechanical properties of the interleaved graphite/BMI fatigue specimens during elevated

temperature fatigue loading. These mechanisms are chemical aging and fatigue damage.

Chemical aging is a thermo irreversible process that is dependent on environment and temperature. Chemical aging includes processes such as continued curing and oxidative breakdown and is driven by exposure to elevated temperature[8]. These two aspects of chemical aging will be discussed in the following pages, as will previous research on the 5260 matrix that demonstrate changes due to continued curing and oxidative breakdown.

Continued Cure Effects

Chemical aging includes continuation of the crosslinking reaction and is considered an extension of the curing. Much work has been done to understand the curing of BMI materials[11-14]. This work relates directly to factors that become evident in elevated temperature testing. Development of damage[31, 32], residual stresses[34, 35], shrinkage[11, 34], and changes in elastic properties[11-14] have been related to cure. It is believed that these changes will affect the fatigue performance of the material.

Insight can be gained into continued curing during elevated temperature testing by explaining the cure cycle the PMC goes through during manufacture. The standard cure cycle for PMC's usually consists of a two step cure cycle[12]. The first dwell is used to consolidate the material into a cohesive solid. The temperature for the second dwell is increased to facilitate crosslinking. Crosslinking is the key to the development of the final properties of the matrix.

The purpose of the second dwell period is to allow the crosslinking reaction of the matrix to occur, thus developing its strength and material properties. The speed, extent of cure, and the properties of the resulting material is highly dependent on the temperature during cure. The higher the temperature, the quicker the crosslinking reaction occurs and the greater the extent of cure. Lower temperature adds to ease of processing but leads to uneconomical cure times. In addition, lower temperatures might not allow the composite to reach as complete a state of cure as higher temperatures.

White and Hahn [11-14] found that for graphite/BMI systems, matrix dominated laminate properties were highly dependent on extent of cure and fiber dominated laminate properties increased moderately with extent of cure. In addition, postcure was shown to increase transverse modulus and strength[11].

However as cure temperature increases so do residual stresses which can cause matrix cracking [13, 34] resulting in decreased strength of the material. In addition, extensive contraction of thermoset matrixes has been reported during the curing cycle[11, 34].

Residual stresses from curing have been determined by analyzing curvature of unsymmetric laminates[13] and by ply separation methods[34]. Studies have related the residual thermal stresses to the extent of cure[11-14, 34-36] and to varying cure temperatures and cycles. These residual stresses can be reduced through the application of pressure during the second phase of cure, although care must be taken not to damage the laminate with this pressure.

Oxidative Breakdown

Elevated temperature studies have demonstrated the tendency of BMI materials to experience oxidative breakdown[34-39]. This breakdown is indicated by continual weight loss during the exposure to elevated temperatures[38]. Because of the ease of the weight loss measurement, attempts have been made to relate it to material performance, although no direct link to material properties is possible[38, 39].

Development of damage due to isothermal aging and thermal cycling is not unusual. Studies of thermo-oxidative stability of the BMI materials at elevated temperatures[34-38] have demonstrated development of edge cracks during elevated temperature exposure. Edge damage provides a site for the damage to initiate and provides more surface area for the oxidative breakdown to occur. Oxidative break down also reduces the toughness of polymeric materials[39]. Changes in the toughness of the interleave region reduce delamination resistance which may result in lower performance in compression after impact (CAI) strength tests. Conversely, increases in the interleave toughness of this region are related to improvement in delamination resistance[15] and CAI response[40]. It is also believed that oxidative breakdown causes the development of damage and changes in the material properties which could increase the damage accumulation during fatigue.

Known responses of the 5260 Matrix

Boyd et al. [41] presented results that show the effect of postcure on the strength on different 5260 systems. The effect of a six hour post cure on compression after impact and open hole compression strength was shown to improve material properties until the aging temperature was raised above 215°C [41]. Martin et al. [42]

showed an increase in E_{11} during the first 1000 hours of aging and an increase in E_{22} until microcracks began to develop. The longitudinal modulus of a $[\pm 45]_{2S}$ laminate was also shown to increase. In another study Tuttle et al. [43] demonstrated an increase in axial stiffness of $[0]_8$ specimens after isothermal aging under load.

Not only can exposure to temperature change the mechanical properties of the material, but it can also cause shrinkage of the material. Martin et al.[42] showed that shrinkage occurred during unloaded isothermal aging. A strain gaged $[30^{\circ}]_{12}$ specimen of IM7/5260 shrank during isothermal unloaded aging at 175°C. Tuttle et al.[43] has also noticed the development of surface damage that appeared as matrix regions in the surface plies shrinking in isothermal long term tests. Composite materials containing 5260 as the matrix material, when exposed to elevated temperature, show changes in material properties and shrinkage as demonstrated by other BMIs during cure.

The 5260 matrix has shown signs of oxidative breakdown after aging at elevated temperatures. Martin et. al.[42] reported extensive cracking of a cross ply laminate after a long-term exposure to a temperature of 175°C after 5000 hours and moderate damage after aging 5000 hours at 125°C. Weight loss was also shown to continually increase during aging at 175°C [42].

The 5260 matrix has demonstrated characteristic effects of curing and oxidative breakdown when exposed to elevated temperatures for extended time periods. These studies on 5260 demonstrated that the process of chemical aging causes changes in the mechanical performance of the PMC when exposed to elevated temperature. It is

believed that these changes will influence the fatigue performance of the OHT specimens.

Fatigue Damage Accumulation Process

The mechanism that is expected to play the greatest role in the degradation in performance during fatigue testing is damage accumulation. As damage accumulates, the stiffness and strength of a laminate will decrease. The damage will accumulate until the stress in the load bearing plies causes fibers to fail, resulting in failure of the laminate. Lower loads will result in longer fatigue lives but also cause greater amounts of damage before failure [19].

There are four basic mechanisms of damage considered in the literature: matrix cracking, delamination, fiber failure, and fiber break with interface debonding. During the majority of the fatigue life of a composite, the dominant damage modes are limited to delamination and matrix cracking[19]. Delamination occurs early in the fatigue life of the composite[32], and is seen as a failure between the laminae when the interface fails. It is caused by the high inter-laminar stresses present in these materials due to their anisotropy. These stresses can be estimated from analytical models[32] and depend highly on the material's properties, stacking sequence, and applied loading. The matrix in a single ply can fail in two different ways, parallel to the fiber and normal to the fiber. The most common form of matrix cracking is the cracking of a layer parallel to the fibers. This is caused by loading perpendicular to the fiber direction or by mismatching Poisson's ratio between layers. Damage can also accumulate normal to

the fiber orientation in the form of micro-cracking and fiber failure. Fiber failure occurs near the end of the fatigue life before the whole laminate failure.

The process of room temperature fatigue failure of an unnotched specimen is explained in many other sources [27, 28], but the general process can be explained as follows. First ply failure is the initial cracking of the weakest ply and usually signifies the initiation of fatigue damage. Next, matrix cracks form parallel to the fiber orientation. These transverse matrix cracks continue to accumulate in the weakest ply until a characteristic crack density is reached. After or during this crack accumulation in the weakest ply, more cracks can begin to develop in the next weakest ply. Cracks in adjacent plies or the same ply can be joined by delamination. Delamination may also form along free edges. Matrix cracks can grow into adjoining layers along free edges and initiate new cracking. The cracks and delaminations continue to multiply. This is continued until some limit of damage is reached and the fibers in the loading direction break causing the failure of the laminate.

The damage results in loss of stiffness. Models have been proposed that relate laminate stiffness to the development of damage [44, 45]. Because of this reduction, stiffness of a laminate has been used to quantify the level of damage in test specimens[7, 19]. Researchers have used techniques such as edge replicate to determine the extent of external damage[1]. By monitoring stiffness and damage along the exposed edges, inferences of internal damage states can be made.

Room temperature effects of damage in open hole specimens are well understood[27,28]. When a stress concentration such as a notch is added, the process is

similar to the unnoched laminate fatigue although the stress concentration will cause damage to propagate faster. This leads to an interesting effect for open hole specimens. As damage increases, delamination and matrix cracking reduce the stress concentration around the hole. This causes an effective "blunting" of the notch resulting in an increase in strength of the specimen from the un-fatigued state.

When fatigue testing is performed on an interleave toughened composite, the toughened material slows damage accumulation. The addition of an interleave slows the initiation and propagation of delamination. Matrix cracking is slowed in its propagation from ply to ply. Since the interleaves slow the accumulation of damage, when an interleaved material contains a stress concentration, the reduction in stress concentration, caused by "blunting", occurs at a slower rate and to a lesser degree[29]. This results in a reduced strength when compared to the non-interleaved composite.

It is believed that the process of aging will interact with the damage accumulation process. These interactions should visible in the residual strength although it is unknown how aging will affect the reduction is the stress concentration caused by damage accumulation.

CHAPTER III

TEST PROCEDURE AND EQUIPMENT

Experimental Program

One type of specimen configuration that has been used to assess mechanical performance of PMCs is the open hole tension (OHT). This is a common specimen configuration which is well suited to studies in which fatigue damage accumulates. One of the advantages of the OHT specimen is that damage accumulates around the area of the strain concentration adjacent to the central open hole. Previous investigations using the OHT test have typically focused on the room temperature fatigue and static behavior, with little data being generated on the interaction of temperature and stress[18, 26-30].

To develop an understanding of the individual effects of temperature and fatigue loading, the experimentation investigation was divided into two parts. The first part consisted of an investigation to determine the effects of elevated temperature and fatigue loading on the response of OHT specimens. The loads and temperatures were varied from relatively benign conditions (low stress, room temperature) up through aggressive conditions (high stress, high temperature). The OHT fatigue investigation provided information on changes in the PMC's stiffness, damage accumulation, and residual properties. The isothermal aging of unloaded OHT specimens allowed comparison of changes in damage accumulation and residual properties caused by the fatigue loading and provided insight into the individual effect of temperature. The second portion of the investigation was an unloaded physical properties study. This

investigation provided information on how unloaded isothermal aging would effect weight loss and the glass transition temperature of the PMC.

Three approaches were used to determine the effect of elevated temperature fatigue on the OHT specimens. First, the stiffness of a gage section centered around the open hole provided information on the mechanical properties of the OHT specimen during the fatigue tests. The monitoring of this stiffness provided insight into the combined effects of damage and aging. Second, the specimen was nondestructively evaluated after the fatigue test to determine the damage accumulation due to fatigue loading or isothermal aging. Careful monitoring of the load induced damage could account for any observed stiffness loss. Finally, the previously fatigued OHT specimens were failed statically to determine effects of fatigue damage and aging on stiffness and residual strength. In order to understand the differences from room temperature OHT fatigue results found in the literature, special emphasis was paid to understanding the individual effects of temperature and stress.

While the OHT investigation provided information on the combined effects of fatigue loading and elevated temperature on the performance of the OHT specimens, the physical properties investigation provided information on how exposure to elevated temperature alone would change the graphite/BMI material during the fatigue tests. The physical properties investigation measured weight loss and changes in glass transition temperature (Tg) as the result of isothermal aging. Measurements to determine the glass transition temperatures were made using thermo mechanical analysis (TMA) and dynamic mechanical analysis (DMA). As outlined in [46], the

measurement of weight loss and Tg can provide information on oxidative stability and chemical aging.

The OHT and physical property investigations provide information on the processes of aging and fatigue damage accumulation. Results from this work will help explain the roles of aging and fatigue damage in the elevated temperature performance of the OHT specimens as well as provide insights into the individual and synergistic contributions of each process.

Test Specimen

Based on ultrasonic C-scans performed at NASA Langley Research Center, the cured panels were determined to be free of manufacturing flaws before machining. Test panels were cured using the manufacturer's recommended procedure. As shown in figure 1, the panels were machined into three specimen types: open-hole tension (OHT), thermal-mechanical analysis (TMA), and dynamic-mechanical analysis (DMA). The DMA specimens were also used to measure weight loss. The OHT specimens were 203.2 mm (8.0 in.) long and 38.1 mm (1.5 in.) wide with a 6.35 mm (0.25 in.) center hole. These specimens were polished on one edge to enhance visual inspection. DMA specimens were 12.7 mm (0.5 in.) wide by 50.8 mm (2.0 in.) long and the TMA specimens were 6.35 mm (0.25 in.) on each side.

After the specimens were machined (and the OHT polished) they were dried for 24 hours at 110°C and kept desiccated until test time.

Strain Field Investigations

The goal of the research was to determine the individual and combined effects of elevated temperature and loading on the OHT specimens. The experimental

program was developed and adjusted to meet this goal. Prior to initiating the fatigue tests, investigations were made into the effect of the center hole on the strain field of the OHT specimen.

Strain field investigations provided information on the strain field around the center hole and how temperature affected this strain field. Two strain field studies were conducted to understand the strain concentration around the center hole of the specimen. The effect of temperature on the stain distribution and stiffness of the laminate was measured in a strain gage study. A full field strain measurement was made at room temperature using a Moiré technique.

Strain Gage

Strain gages were mounted on an OHT specimen as shown in figure 2. In addition, an extensometer, as used in the fatigue tests, was mounted on the edge to understand the relation between the strain measured at the specimen edge and the strain across the width. The 25.4 mm (1 in.) gage length extensometer was mounted centered on the 6.35 mm (.25 in.) hole.

Static tests were performed at different test temperatures to understand the effect of temperature on the strain field. The specimen was loaded at a rate of 22.2N/sec to 13300N (3000 lbs.). Strain measurements were taken every 20 seconds. Tests were performed at nine temperatures from 23°C to 204°C. (23, 38, 66, 93, 121, 149, 163, 177, 204°C)

Strains measured at the extensometer and those measured by strain gages at locations 1, 4, 6 were found to agree to within 8% over the entire temperature range.

All strains gages away from the hole (1, 4, 5, 7) were also found to be linearly proportional to strain measured by the extensometer. This demonstrated that the extensometer gave good strain readings in the gage section that were representative of strains away from the center hole.

Moiré

The Moiré technique was used to provide visualization of the strain field around the center hole. An array with a frequency of 2400 lines/mm was applied to the surface of the specimen. Load was applied at room temperature to the specimen using a screw driven load stand. Pictures of the Moiré fringe pattern were produced with a 35mm camera that allowed calculation of the axial strain field using equation 1.

$$\varepsilon = \frac{1}{f}\left(\frac{\Delta Ny}{\Delta y}\right) \tag{1}$$

where: f = frequency of array

ΔNy = Change in fringe number (i.e. number of fringes)

Δy = Change in axial distance (distance covered by ΔNy fringes)

A more detailed explanation of the theory and procedure used for Moiré can be found in reference[47]. Figure 3 shows the fringe pattern for a OHT specimen loaded to 81.1 MPa. The fringe pattern in figure 3 indicates that the effects of the stress concentration are minimal at the specimen edge and that the strain field at the edge is almost uniform. Therefore, it was assumed that the strain measurement taken from the extensometer, which attaches to the edge, will not be adversely effected by the stress concentration. The fringe pattern of figure 3 also shows that the effects of the stress concentration caused by the notch are all contained in the 25.4 mm (1in.) gage section.

Therefore is was further assumed that most of damage induced by the stress concentration would occur in the gage section.

Open Hole Tension Testing

Tests were performed to determine the effect of elevated temperature on the fatigue and static residual properties. A range of load levels and test temperature were used to evaluate the material's performance.

The tension fatigue tests were performed on a 222 kN (50 KIP) capacity servo-hydraulic test stand. Load, strain, actuator displacement and time were recorded using an automated digital data acquisition system. An environmental chamber equipped with a viewing window maintained the temperature of the grips and specimen. A long focal length microscope allowed inspection of the specimen through the oven window.

Alignment and Calibration

Before testing, the servo hydraulic test stand was aligned and calibrated using standard laboratory practices. Measurements were taken to insure proper alignment of the test stand. Alignment was checked using a strain gaged aluminum specimen. The load cell was calibrated for numerous ranges before testing began. This provided a resolution of 5lb for the 12-bit data acquisition board. The extensometer was also calibrated for a .01 in. range before testing. This provided a resolution of 5 micro-strain (με) for the 12-bit data acquisition board.

OHT Testing Conditions

All open hole tension fatigue tests were performed under load control at a frequency of 1 Hz. with a min./max. stress ratio of R=0.1 and a triangular wave form.

A minimum of two tests were performed at each condition and tests were concluded after 400,000 cycles. This test matrix is summarized in table 1.

In addition to the fatigue load tests, a set of tests were conducted on open hole specimens that were aged without load in a oven at the fatigue test temperatures for 120 hours. This aging time was equivalent to the fatigue time. These tests provided information on how the properties of the OHT specimens were affected by elevated temperature without load. The specimens were subjected to the same residual property tests and damage investigation as the fatigued specimens.

Fatigue loads were chosen to represent a moderate and an aggressive condition. Two maximum far field stresses were used, σ_{max} = 119 MPa (17.25 ksi.) and σ_{max} = 238 MPa (34.5 ksi.) which corresponded to 23% and 46% of ultimate strength, respectively. Stresses were calculated using the area of the unnotched cross section. These stress levels also corresponded to far field strains of 0.2% and 0.4% strain respectively. The 0.4% is the maximum allowable design strain for many of these new composite materials[48].

Test temperatures were chosen to represent a range from benign to aggressively high temperatures. Tests were performed at 23°C (room temperature), 177°C (350°F), 191°C (375°F), 204°C (400°F), and 218°C (425°F). The room temperature tests provided baseline information. The next highest temperature, 177°C, was chosen to correspond to a high use temperature. The 191°C temperature corresponded to the temperature during the second step of the cure cycle. The higher temperatures were chosen to provide information on accelerated test conditions. It is also interesting to

note that the highest temperature chosen corresponds to the temperature suggested by the manufacturer for the six hour recommended post cure cycle.

Mechanical Properties Procedure

Prior to testing, the specimen was centered and squared in the mechanical grips using preset alignment guides. A 101.6 mm (4 in.) gauge section between grips was used with 50.8 mm (2.0 in.) in each grip. The specimen was oriented in the environmental chamber to allow visual inspection of the polished edge using the long focal distance microscope. A 25.4 mm (1.0 in.) gauge length, high temperature, capacitance extensometer was centered on the 6.35 mm (0.25 in.) hole and edge mounted on the unpolished side. Specimens were heated to test temperature and held for 30 minutes before cycling started to allow for thermal equilibrium.

The measurement of strain and load occurred during specified cycles of the fatigue test and allowed determination of longitudinal stiffness changes. Readings occurred logarithmically (1,2,5,10,20...) until 100,000 cycles were reached and then every 100,000 cycles until the end of the test at 400,000 cycles. During some of the later tests readings were taken logarithmically until 5,000 or 10,000 cycles and then continued every 5,000 or 10,000 cycles.

Mechanical Properties Analysis

The effect of fatiguing on the mechanical properties of the specimens was determined from the load and strain test data mentioned above. Stiffness changes have been used as an indicator of internal damage [7, 19]. For the current work the stiffness changes reflected the effect of damage and aging over the one inch gage section.

Stiffness calculations were performed by making a least squares linear fit to the stress and strain data as shown in figure 4. Stress was calculated using the unnotched specimen area and the load from the data acquisition system. Strain was taken from the extensometer attached to the gage section. The fit was performed on the loading and unloading data between 5% and 95% of the maximum load for that fatigue cycle. This provided an effective stiffness for the notched gauge section.

Once the stiffness had been calculated, it could be plotted as a function of cycle counts or aging time for each fatigue test. To aid in comparison of data, all fatigue stiffness data was normalized with respect to the initial stiffness (i.e. the stiffness at cycle count, N=1). This allowed comparison of fatigue tests over a range of temperatures which would have otherwise masked the small changes induced by damage and aging. The strain gage study showed that the laminate stiffness decreased 7.9% when the temperature was raised from 23°C to 204°C. This change was of the same magnitude as any changes due to damage or aging during a single isothermal fatigue test.

Plotting the normalized stiffness gave an indication of the change in stiffness over the duration of the fatigue test as shown in figure 5 and figure 6 Both of these figures show the results for a single fatigue test conducted at a temperature of 218°C with a maximum load of 119 MPa. Both plots show the normalized stiffness of the gage section plotted against the cycle count. Figure 6 shows this on a linear scale. Figure 5 shows the same data on a semi-log representation where the normalized stiffness is plotted against the log of the cycle count.

Stiffness measurements were grouped into three regions depending on the rate of change of stiffness. The first two linear regions are easily visible on the semi-log plot. While third linear region is most easily seen on the linear plot. Fits were performed to these regions to aid in the visualization of data. The first two fits were conducted by performing least squares reduction (LSR) fits to the semi-log data. The third fit was conducted by performing a linear LSR fit to the normalized stiffness vs. cycle count. Fatigue data will be presented in the results section with three fits on the semi-log plot.

Average results for each test temperature and loading were needed to compare the effects of the different test variables. This was complicated by irregular sampling rates during the execution of the test matrix. The fits facilitated average results calculations for each set of test conditions. Once regions were selected, these three fits represented each test by the same number of variables. Average test results were then calculated by taking the average of the fits for each range. Results from three fatigue tests for one set of testing conditions are shown in figure 7 along with the average for the condition (plotted as a solid line). Calculating the average of the fits resulted in the equal weighting of each individual fatigue test independent of the sampling rate.

Fatigue Damage Investigation Procedure

The damage investigation of the fatigued specimens consisted of two portions: an in-situ investigation and a post test examination. The in-situ investigation was performed to provide information on the extent of damage as the fatigue tests progressed. A monitoring technique was developed to provide visual inspection of

damage in the environmental chamber. After the completion of the fatigue test, a detailed investigation of the damage was made. The post-test damage investigation was performed to determine the extent of damage without affecting the residual mechanical properties of the fatigue specimens. This detailed investigation included inspection of edge replicates, x-ray radiographs and photo micrographs.

During the test, inspections of the polished edge of the test specimen were made periodically with a long focal length microscope to access damage. These inspections were performed with the oven closed; the glass window in the oven door provided a viewing port. Fiber optic light sources mounted in the oven were adjusted for proper lighting. The output from the microscope's CDC camera was recorded using a VCR to provide a record of observations. Before each test was started, base line images were taken to determine any initial damage.

Video recordings of the edge were performed on the one inch gauge section. This allowed inspection for transverse matrix cracking and delamination to be performed during the test. These recordings were made after the data acquisition system had taken a stiffness reading which allowed correlation of stiffness with edge damage. Due to the extent and nature of the damage, this procedure did not provide the useful information expected (explained in the results section). The in-situ damage investigation procedure was not performed during the later tests which allowed for greater sampling frequency. This was possible because the data acquisition was automated and did not require a person to perform data collection .

The post-damage evaluation included three inspection procedures. The first inspection consisted of making an edge replicate of the gauge section to determine the extent of matrix cracks and to compare crack density to the video image made during in-situ inspections. The edge replicates were performed on the polished edge of the unloaded test specimens. A small amount of acetone was placed on the polished edge. A piece of replicate material (acetate) was then placed over the gage section. This provided an accurate reproduction of the edge that could be viewed in a microfiche reader or microscope. The number of transverse matrix cracks in each ply along the gauge section were recorded.

The second inspection, a visual investigation, was made of the polished edge using a microscope. This investigation was made to find characteristic damage patterns or surface characteristics that might be associated with the temperature and/or loading conditions. Magnifications raged from 60X to 1500X. Photographs were taken using Polaroid Type 53 Instamatic Land camera film at different magnifications. Damage measurements of transverse matrix cracks in each ply were again recorded for the entire gage section.

Finally, X-ray radiographs, were made to investigate the internal damage. A zinc iodine die penetrant was used with the composite specimen. This penetrant was placed on the edge of the specimen and the specimen was gently flexed and then allowed to set. Then the specimen was placed on Polaroid Type 53 Instamatic Land camera film and the x-ray radiographs were made under no load. These radiographs were inspected for evidence of possible delamination and depth of matrix cracking.

Fatigue and Isothermal Aging Damage Analysis

This investigation of the OHT specimens was made to find damage associated with the temperature and/or loading conditions. The in-situ damage investigation allowed observation of general laminate edge condition. Attempts were made to correlate this with internal damage. Edge replicates provided basic post-test damage estimates. Total cracks per inch and cracks per ply orientation per inch were calculated. The edge replicate allowed easy measurement of matrix cracking.

Although the edge replicates showed edge damage, a microscope was also used to view the edges of specimens. It was found that microscopic inspection provide a clearer picture of damage than the edge replicates. A sample picture from the microscope and an edge replicate are shown in figure 8. The microscopic inspection not only provided more accurate information on edge matrix cracking but also showed changes in the surface characteristics due to temperature and loading.

The x-ray radiographs were the most useful measurement of damage since they allowed insight into the internal damage state of the laminate. Information was provided on general matrix cracking in the laminate and damage located around the center hole. Matrix cracking, delamination and axial splitting could all be measured from the x-rays. The extent of damage provided insight into changes in stiffness and residual properties.

Residual Properties Procedure

After investigation for post-fatigue damage, the specimens were loaded in static tension until failure at room temperature. This allowed a comparison of the different

fatigue or isothermal aging conditions on the remaining strength, stiffness and ultimate strain of the material.

The static tests were performed on a 88 kN (20 KIP) servo-hydraulic test stand equipped with an automated data acquisition system. The specimen was centered and squared in the hydraulic wedge grips using preset alignment guides. A 127.0 mm (5 in.) gauge section between grips was used with 38.1 mm (1.5 in.) in each grip. Tests were performed in stroke control at a ramp rate of 1 mm/min (.025 in./min). This speed was chosen to insure an entire test time between 1 and 10 min. for all tests. Two 25.4 mm (1 in.) gauge length extensometers were mounted on the edges and centered with respect to the hole to provide strain data. Load and strain were recorded on half second intervals during the test. All static tests were performed at room temperature and continued to failure.

Residual Properties Analysis

Residual properties calculations and analysis are illustrated in figure 9. Residual properties calculations consisted of ultimate strength, ultimate strain, and secant modulus. Ultimate stress was calculated using the area of the unnotched cross-section and the highest load carried by the laminate. Ultimate strain was measured as the largest strain carried before failure. The secant modulus was calculated between the values of 1000με and 3000με.

Physical Properties Testing

The effects of aging at temperature on the composite material during the fatigue testing was determined through a physical property investigation. The physical

properties that were measured consisted of weight loss and glass transition temperature (Tg).

Physical Properties Test Conditions

Physical property measurements were performed after every 24 hours of aging for five days at all fatigue testing temperatures. Tests were performed at 23°C (70°F), 177°C (350°F), 191°C (375°F), 204°C (400°F), and 218°C (425°F). Two TMA and DMA specimens were used for each time and temperature condition. Test conditions are summarized in the test matrix shown as table 2. TMA and DMA were both used to determine Tg before and after aging. Glass transition temperature tests were run on specimens that had been dried but not exposed to any additional thermal history to provide unaged Tg measurements.

Weight Loss and Glass Transition Procedure

After drying and prior to testing, DMA specimens were removed from the desiccator and weighed to within ±.00001g using an analytic balance. The ovens were open for the period of time required to remove the specimens and then closed immediately, causing only a minor temperature fluctuation. After completion of the aging, the DMA specimens weighed to determine weight loss. After weight loss was measured, the TMA and DMA tests were performed to calculate T_g. Weight loss was calculated using equation 2 and was plotted as a function of aging time for all test temperatures.

$$W_{loss} = \frac{W_{initial} - W_{final}}{W_{initial}} \times 100\% \qquad (2)$$

TMA tests were conducted with a 50.0 mN load. The material was heated from room temperature to 400°C at a rate of 10°C/min. Glass transition was taken as the point were the coefficient of thermal expansion (CTE) of the material changed. The Tg was taken at the first major inflection point on the deflection vs. temperature plot. Figure 10 shows TMA results for T= 191°C and t=72 hours. Tg was calculated to occur at 317.75°C in figure 10. In addition to Tg, CTE was calculated for the material between the temperatures of 75°C and 175°C.

DMA tests were also conducted to determine Tg. DMA tests were performed from room temperature to 400°C at a rate of 5°C/min. Glass transition temperature was taken as the peek of the tan delta curve. Figure 11 shows DMA results for T= 219°C and t=96 hours indicating that the Tg occurred at 293.7°C.

Table 1. Number of fatigue tests at each condition.

Temperature	Stress Level σ_{max} = 119 Mpa	σ_{max} = 228 Mpa	Base Line No Load Aged 120 Hours
23°C	2	2	2
177°C	2	2	2
191°C	2	2	2
204°C	2	2	2
218°C	2	2	2

Table 2. Number of physical property tests at each condition.

Time (Hours)	Test TMA	DMA	Weight Loss
0	2	2	-
24	2	2	2
48	2	2	2
72	2	2	2
96	2	2	2
120	2	2	2

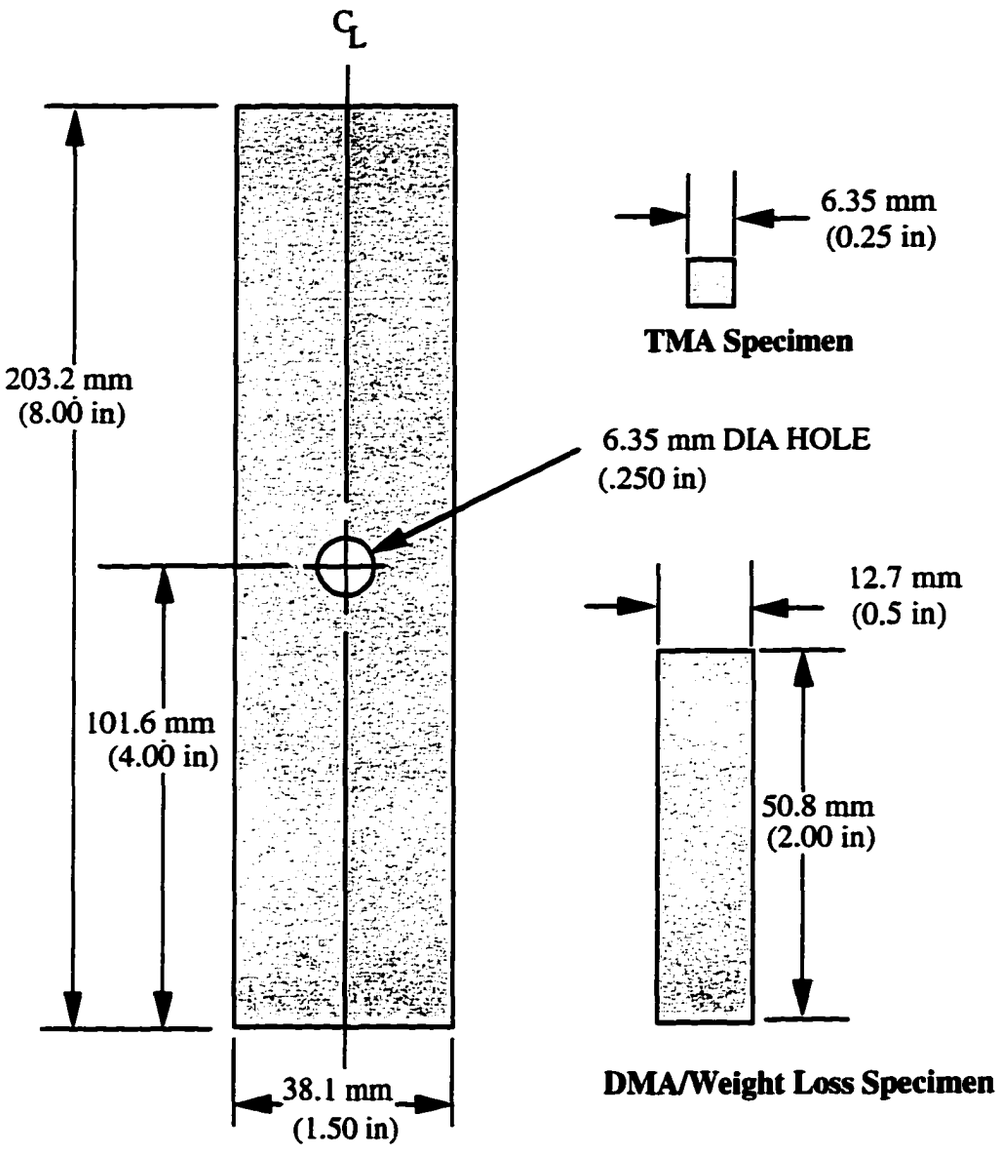

Figure 1. Specimen configurations.

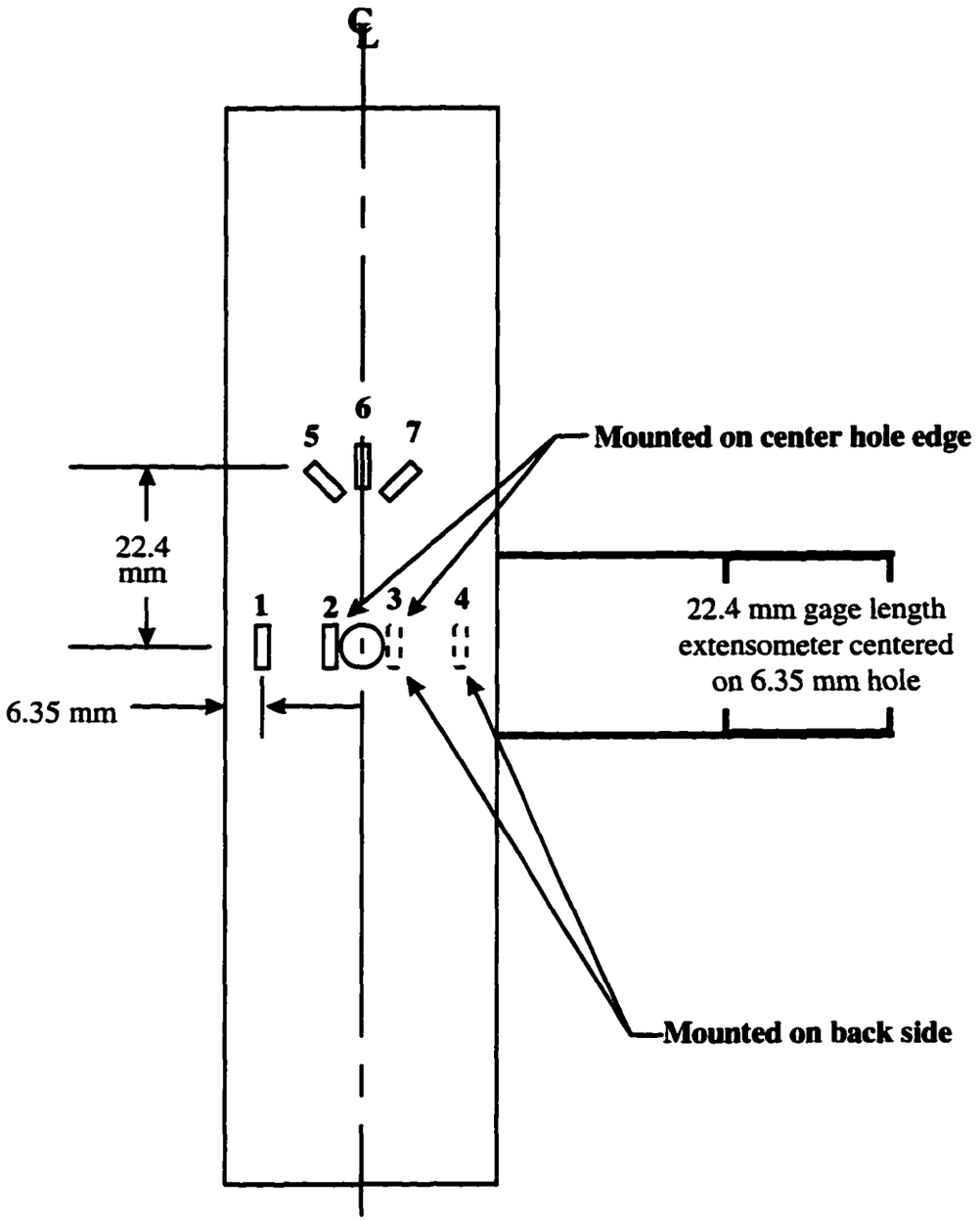

Figure 2. Strain gage and extensometer placement on OHT specimen used for strain field study.

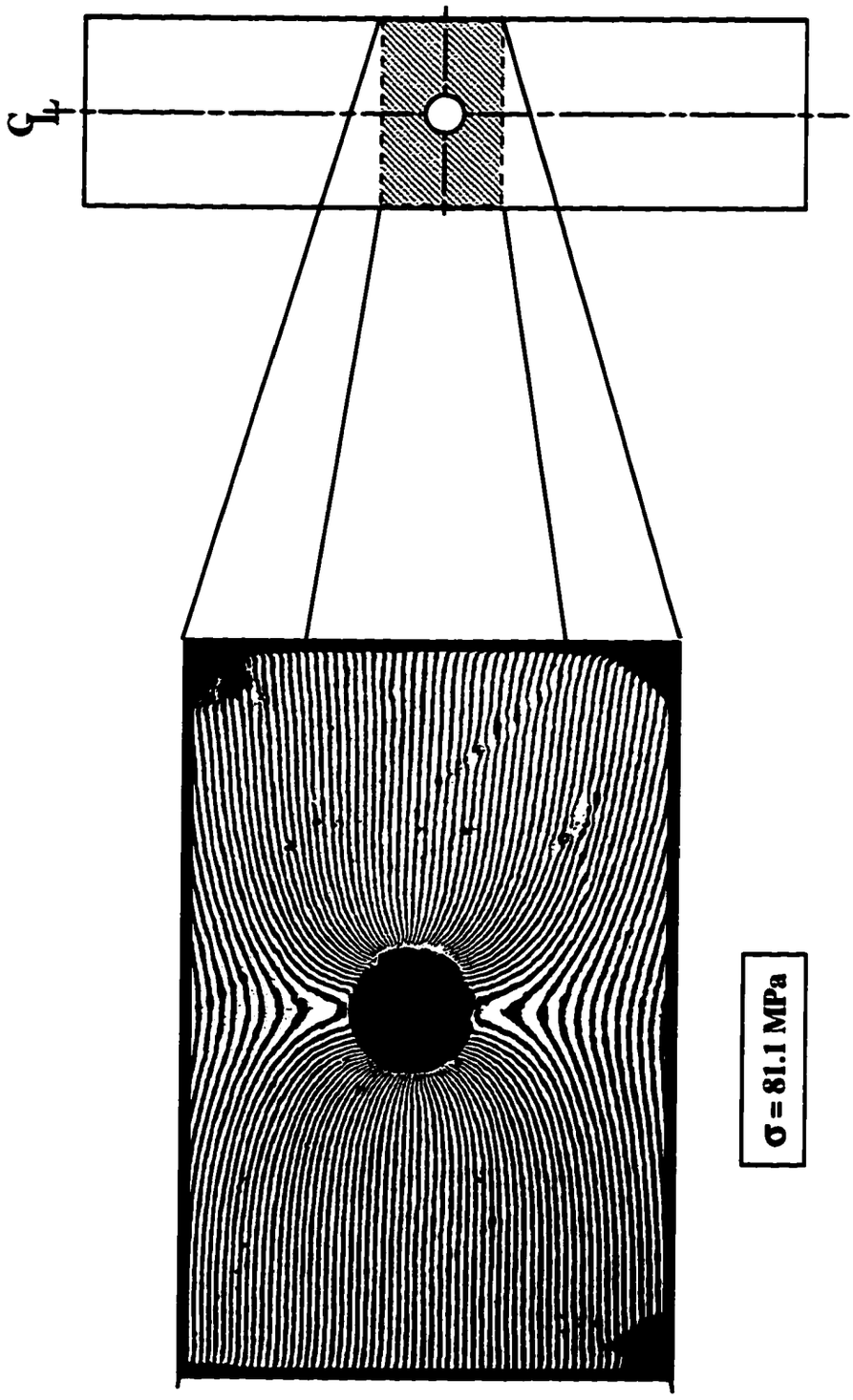

Figure 3. Moiré results showing the extensometer gage section.

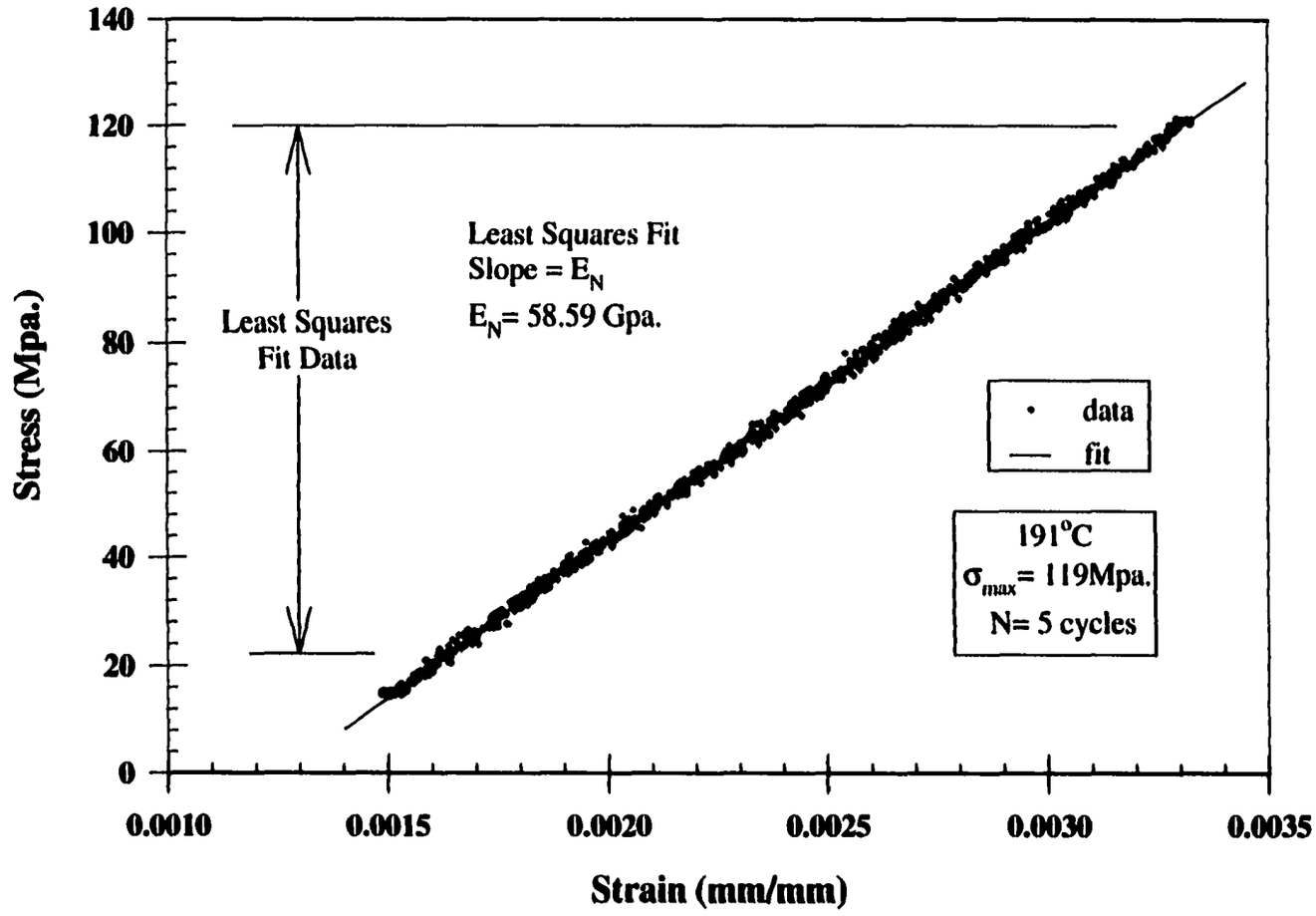

Figure 4. Least squares reduction analysis of a single fatigue cycle data.

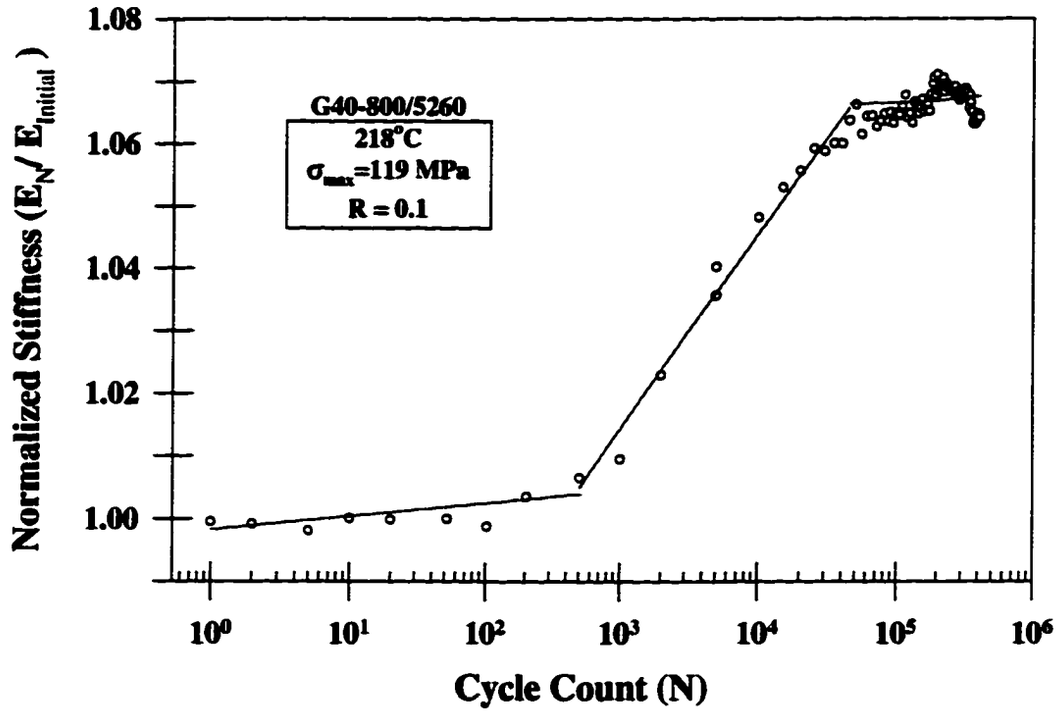

Figure 5. Normalized fatigue stiffness of OHT specimens plotted as a function of the log of the cycle count.

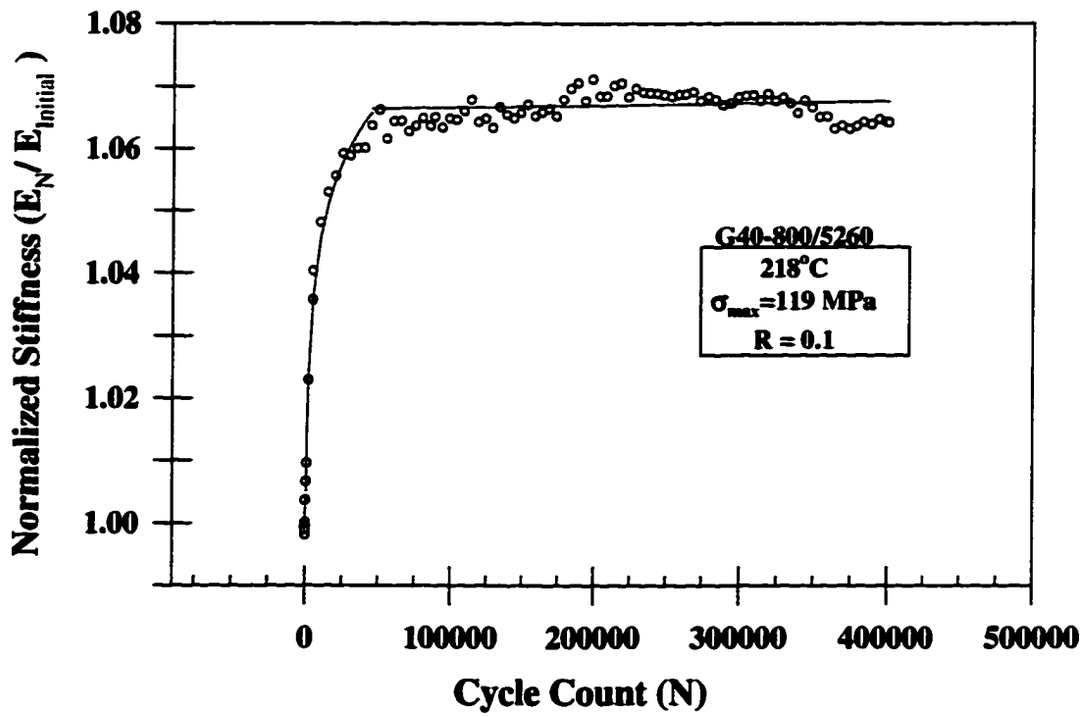

Figure 6. Normalized fatigue stiffness of OHT specimens plotted as a function of the cycle count on a linear scale.

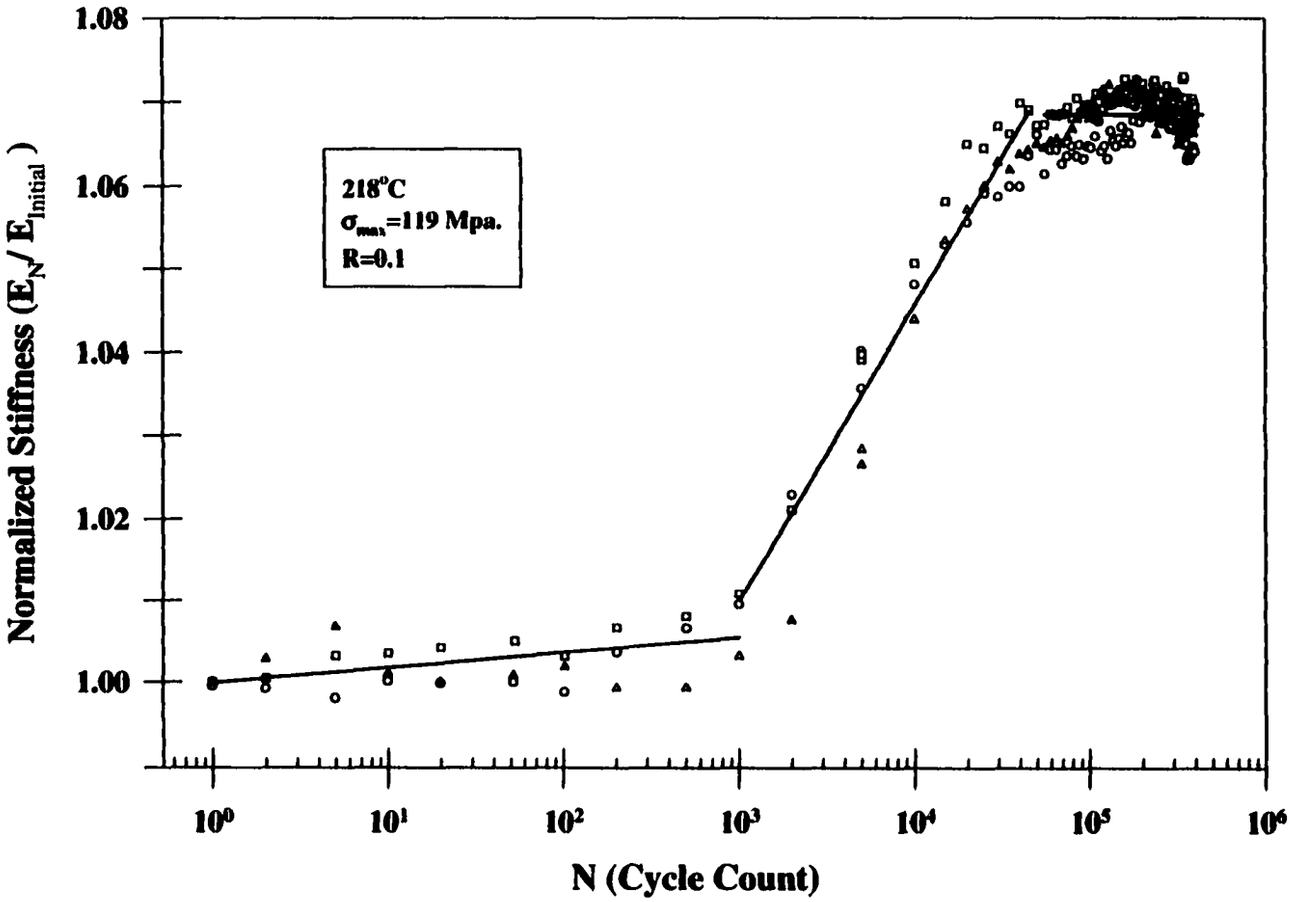

Figure 7. Normalized fatigue stiffness plotted for three 218°C, 119 MPa tests along with the condition average fit.

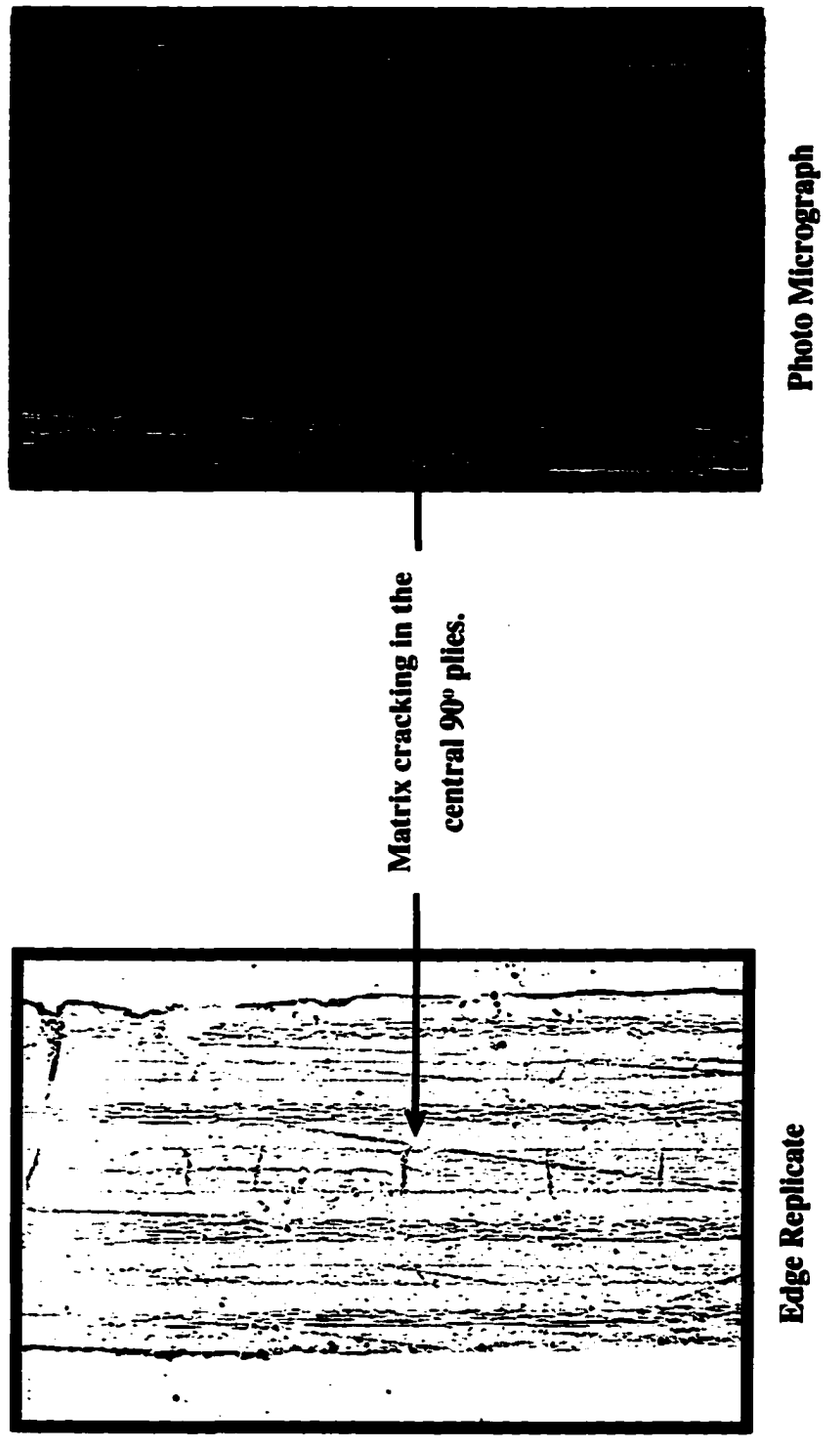

Figure 8. Edge replicate and micrograph showing a comparison of detail.

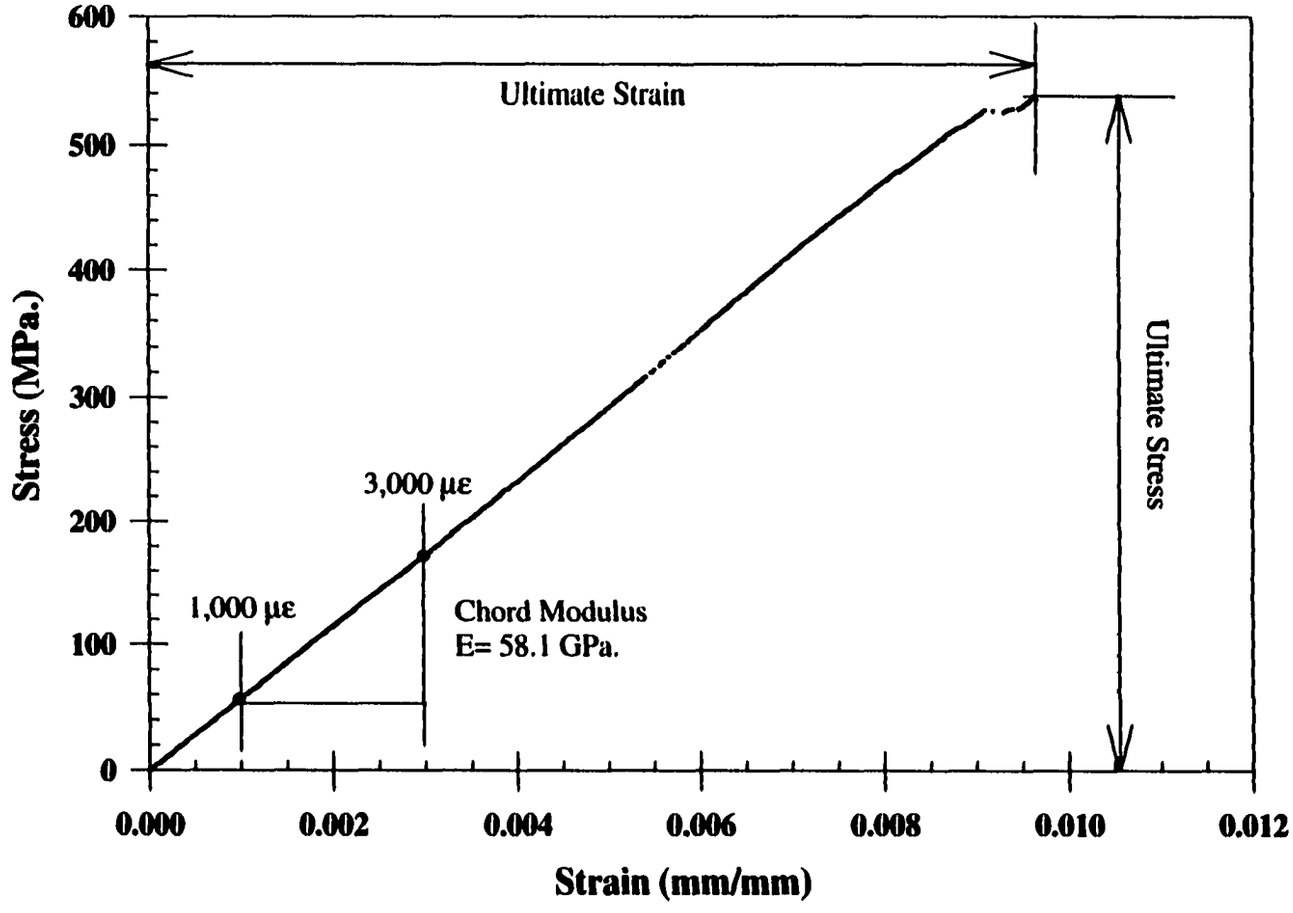

Figure 9. Static test results shown with measured and calculated quantities.

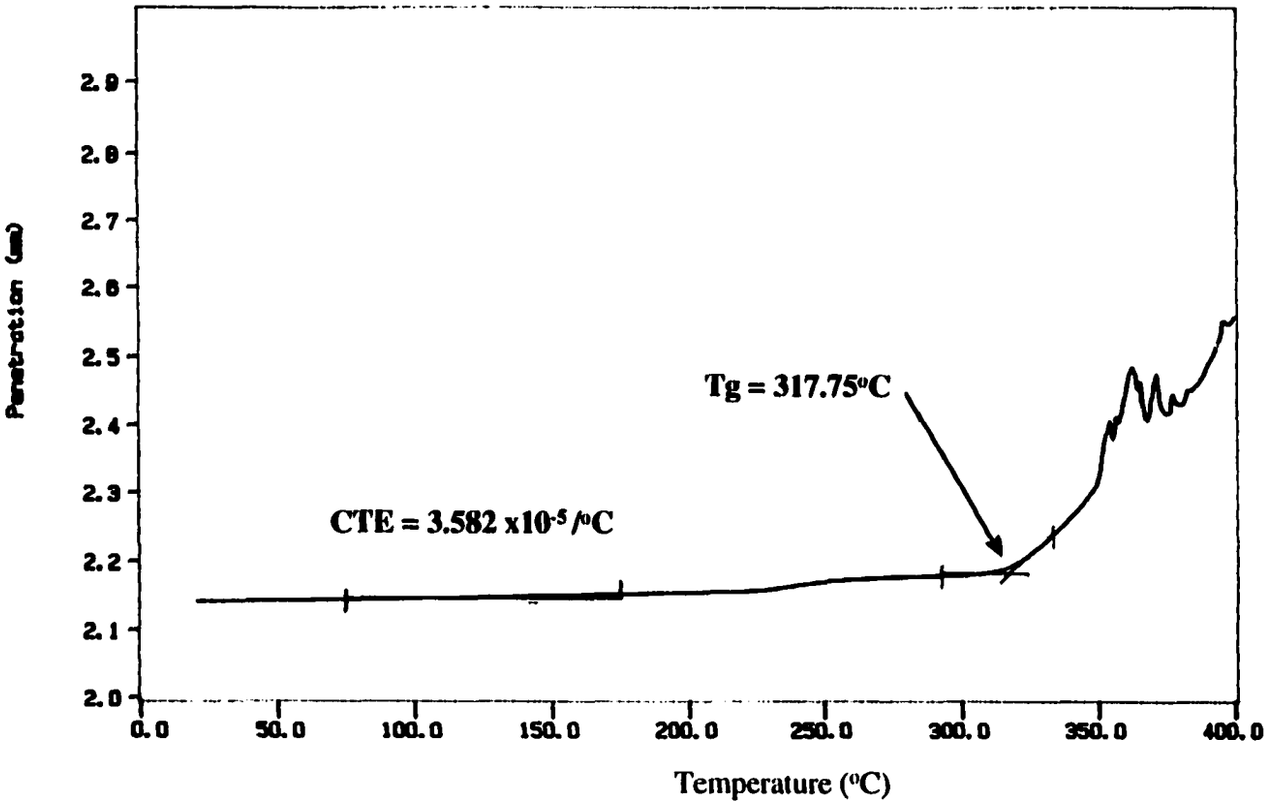

Figure 10. TMA results showing the glass transition temperature and coefficent of thermal expansion.

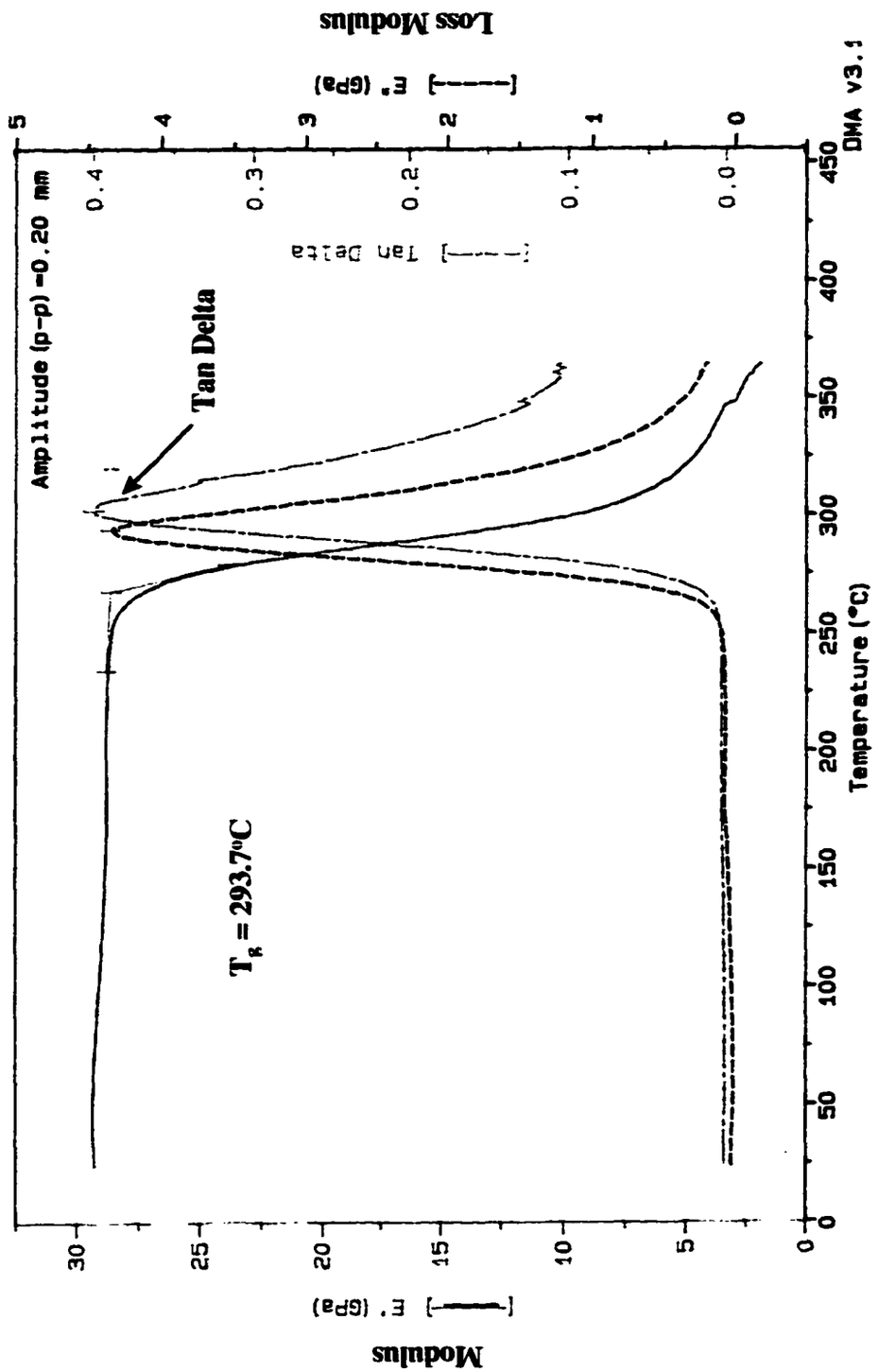

Figure 11. DMA results showing the glass transition temperature as a peek in the tan delta curve.

CHAPTER IV

EXPERIMENTAL RESULTS

Physical Properties Investigation

Weight Loss

Measurements of weight change after isothermal aging without mechanical load were made at all test temperatures to determine the extent of oxidation or loss of volatiles occurring over the 120 hour test period.

The results, shown in figure12, indicate that weight loss does indeed occur at all temperatures and that there are distinct differences due to aging temperature. The figure shows the percent weight loss as a function of the aging time for each of the four elevated testing temperatures. Two replicates were used for each measurement. Figure 12 indicates that very little scatter was observed in the weight loss data.

As temperature is increased so is the weight loss which is demonstrated by comparing the final values shown for each temperature. For the lower test temperatures, 177°C and 191°C, a constant level of weight loss was obtained after the first 24 hours of aging and maintained for the remaining portion of the 120 hour test. At 204°C and 218°C the amount of weight loss continued to increase throughout the duration of the test.

Tg Results

Further evidence of material property changes due to aging was given by measurements of changes in T_g of the composite after 120 hours of isothermal aging. Figures 13 and 14 show the measured values for Tg during aging for the 120 hour test

duration. The first shows the glass transition temperatures provided by the DMA tests, and the second shows the glass transition temperature measured from the TMA tests. Although the specific values change depending on the testing measurement (higher for DMA as expected) the trends are similar.

As shown by the DMA results in figure 13, the Tg increased after aging at all of the fatigue test temperatures. Glass transition results for the DMA were taken as the peak in the tan delta curve. Unfortunately, the 204°C and the 177°C specimens were exposed to ambient conditions for several days prior to measuring the Tg. The moisture gain during this time may have caused the Tg of the material to decrease.

Open Hole Tension Investigation

The open hole tension investigation consisted of three areas of investigations for the aged and fatigued OHT specimens. The first area was the extensive post fatigue/aging damage investigation and the in situ damage investigation. Unfortunately, the in-situ investigation yielded very little useful information. The second area of investigation was determining the mechanical condition of the OHT specimen during the tests. As mentioned in the procedures, the mechanical properties of the OHT specimen were monitored by stiffness measurements of the gage section. The third area of investigation was the effect of the aging/fatigue time on the residual properties of the material.

The results are presented in this order so that damage information can be used to help explain later fatigue results and residual properties results.

Damage Investigation Results

The post aging/fatigue damage investigation consisted of two parts: a visual inspection of the edge of the laminate that provided information on matrix cracking and an x-ray radiograph that provided information on internal damage. In addition to an investigation for damage, a visual study of the aged OHT specimens was made to determine the effects of temperature

Edge damage was measured optically over the 25.4 mm (1 in.) gage section of the fatigued and aged specimens. The post-test damage investigation revealed that most visible edge damage consisted of cracks in the 90° plies. The extent of edge damage (crack density) in these plies are summarized in figure 15. This plot shows the average number of cracks per millimeter in 90° plies of the gage section. The data is presented for all three loading conditions, (no load, 119 MPa, and 238 MPa) and all five test temperatures.

For the no load condition, matrix cracks were not detected for aging temperatures below 191°C. Despite the absence of load, edge cracks developed at 204°C and 218°C. The room temperature specimens fatigued at the low stress level also showed little or no matrix cracking. For all three loading conditions it was observed that as test temperature was raised the number of cracks per millimeter increased. The highest crack density occurred at the highest stress level and highest temperature. At the higher temperatures, (204°C and 218°C) extensive matrix cracking was present for isothermal aging and both fatigue loading conditions.

X-rays were performed on the OHT specimens after they were fatigued or isothermally aged. The internal damage is shown in x-ray radiographs in figures 16-20. Each of these figures shows the x-ray results for one test temperature. The high(a) and low(b) fatigue load tests are both shown in each figure. The radiographs of the isothermally aged specimen which showed no internal damage are not shown.

The specimens that experienced the higher fatigue stress showed the most extensive internal damage. Matrix cracking, axial splitting and delamination were all visible in x-rays of the high stress case. Internal damage did not increase with the increase of test temperature as the edge damage implied. The most extensive damage was visible in the specimen tested at room temperature. At room temperature, the matrix cracks extended from the free edge towards the center hole and from the center hole to the edge. The length of these cracks decreased as temperature increased (Fig. 16a-20a).

The unloaded and low fatigue stress level tests produced very little internal damage that could be detected from the radiographs. The unloaded specimens showed no internal damage. The low load damage did not vary noticeably with temperature and consisted mainly of a very small area of matrix cracking and delamination around the center hole (Fig. 16b-20b).

Matrix cracking was not visible on the x-rays (Fig. 16b-20b) even though it was highly visible during the edge investigation. Internal matrix cracking was visible on other x-ray radiographs when they were of relatively short lengths.

The in-situ damage investigation was conduced to correlate stiffness loss with damage. This was based on the premise that edge damage would provide information on the internal matrix cracking and this could explain any loss in stiffness. This research could have been used correlate experimental data with a damage mechanics model such as the one developed by Harris, Allen and Coats[1-5]. Since it was found that edge damage did not represent internal damage, the in-situ damage investigation was abandoned. The matrix cracking in the video image was usually slightly visible after the after 48 to 72 hours. As the testing continued the edge damage became more and more defined. This damage did not correlate well with internal damage, loading, or changes in stiffness.

Fatigue Stiffness Results

Using the isothermal stiffness measurements taken during the fatigue tests, the effects of stress level and test temperature were examined. The format for presenting all of these results are plots of normalized longitudinal modulus versus the log of cycle count. Each data set represents an average of a least two replicates. The test data for individual tests is show in the appendix-1. To facilitate examination of the effects of temperature on stiffness changes during fatigue, condition averages for all temperatures were plotted for each stress level. Figure 21, was for the low stress level cases while figure 22 was for the higher stress case.

The low stress level cases shown in figure 21 illustrate the dependence of stiffness on test temperature. In a manner similar to the room temperature data of [1], the lower two test temperatures show a total net loss in stiffness over the fatigue test

duration. As the temperature was raised, the rate of stiffness change (after the first 1000 cycles) increased. The data in figure 21 indicates that as the temperature is increased so is the rate of stiffness change. The largest rate and total increase in stiffness was associated with the highest test temperature, 218°C.

For the high stress case, the data given in figure 22 also indicates that as the temperature is increased so is the rate of stiffness increase. The lower two test temperatures show a total change in stiffness similar to the low stress condition. The lower two test temperatures show a loss in stiffness as expected by traditional fatigue results during the first 1000 cycles. However, by the end of the test the stiffness had almost returned to its initial value. Until the last segment of the test, the 177°C specimens yielded a higher normalized stiffness throughout the test than the room temperature specimens. As the temperature was raised above 177°C the rate of stiffness change continued to increase. The largest net increase (and lowest initial drop) in stiffness occurred during the 218°C test due to the effects of aging.

Figures 23-27 show the high and low load level results for each test temperature. The effects of stress level during fatigue are shown in table 3. Results of the test that was conducted at the highest test temperature, 218°C, illustrate the effect of fatigue load level and are given in figure 23. Comparing the results for the two stress levels reveals that the higher stress resulted in an increased rate of stiffness loss during the initial 1000 cycles and increased rate of stiffness gain during the final portion of the fatigue test.

Residual Properties Results

Residual property static measurements were made after the completion of the fatigue tests to determine the effects of temperature and fatigue loading on the remaining specimen strength and stiffness. All of these tests were conducted at room temperature and included the isothermally aged baseline (not fatigued) specimens for comparison. Data is plotted for all five test temperatures and all load cases.

Residual strength was taken as the maximum load carrying capability of the laminate during the course of the static test and is explained in the procedure section. Examination of the data in figure 28 reveals that the highest strength was associated with the room temperature, high stress case, while the lowest strength was associated with the high stress, next to highest temperature case. Both high and low stress cases show decreasing strength with an increase in fatigue test temperature. The baseline strength values were unaffected by temperature and slightly lower than most of the strength values for the fatigue tests. These changes in strength due to stress and temperature are similar to results found by Boyde[41] while researching post cure cycles for the 5260 matrix material.

Residual stiffness in the gage section was unaffected by the fatigue stress level or temperature (Fig. 29). The results for all cases were similar to the baseline test values.

Table 3. Rate of stiffness change in age section for different fatigue load and temperatures

Temperature	σ_{max} = 119 MPa % increase in normalized stiffness per decade increase in cycles	σ_{max} = 238 MPa % increase in normalized stiffness per decade increase in cycles	σ_{max} = 119 MPa % increase in normalized stiffness per 100,000 cycles	σ_{max} = 238 MPa % increase in normalized stiffness per 100,000 cycles
23°C	-0.16	-0.20	0.02	0.17
177°C	-0.07	-0.08	0.03	0.06
191°C	-0.08	-0.15	0.16	0.13
204°C	0.12	-0.02	0.06	0.19
218°C	0.08	-0.20	-0.08	0.55
range	$N \leq 2000$		$100{,}000 \leq N$	

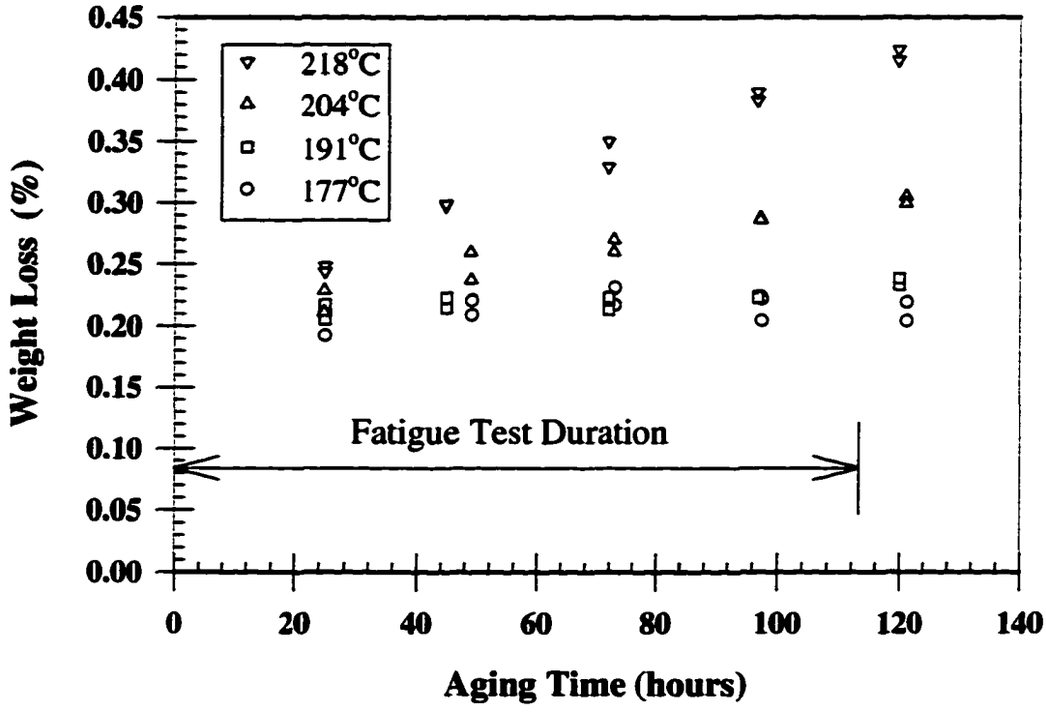

Figure 12. Weight loss plotted as a function of aging time.

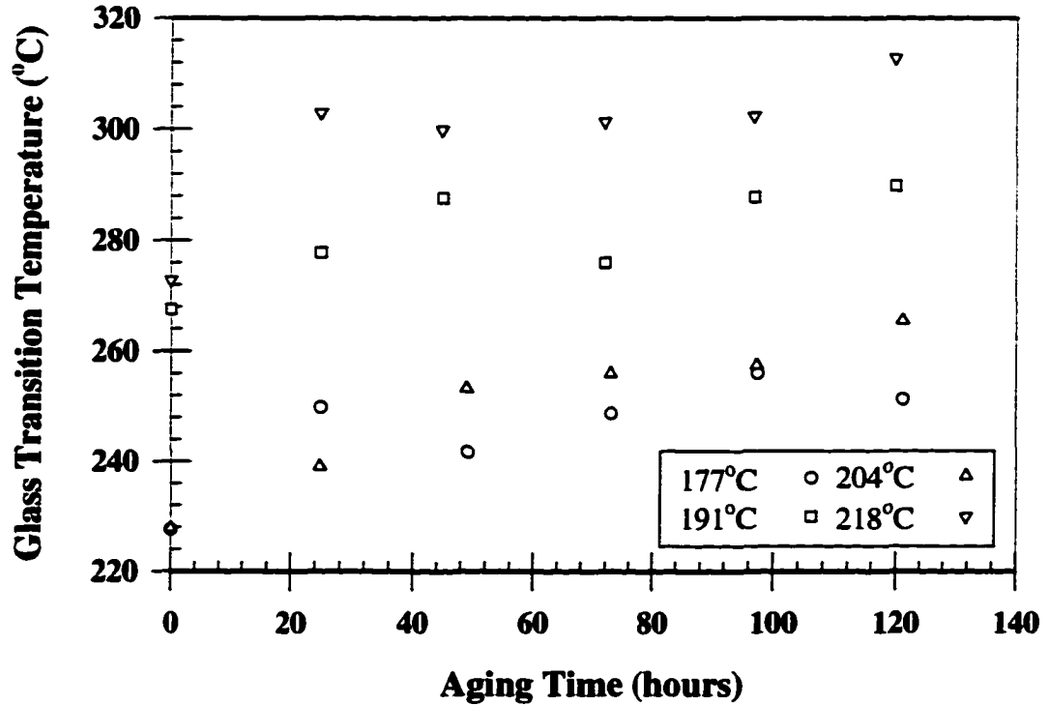

Figure 13. Tg as measured with DMA plotted as a function of aging time.

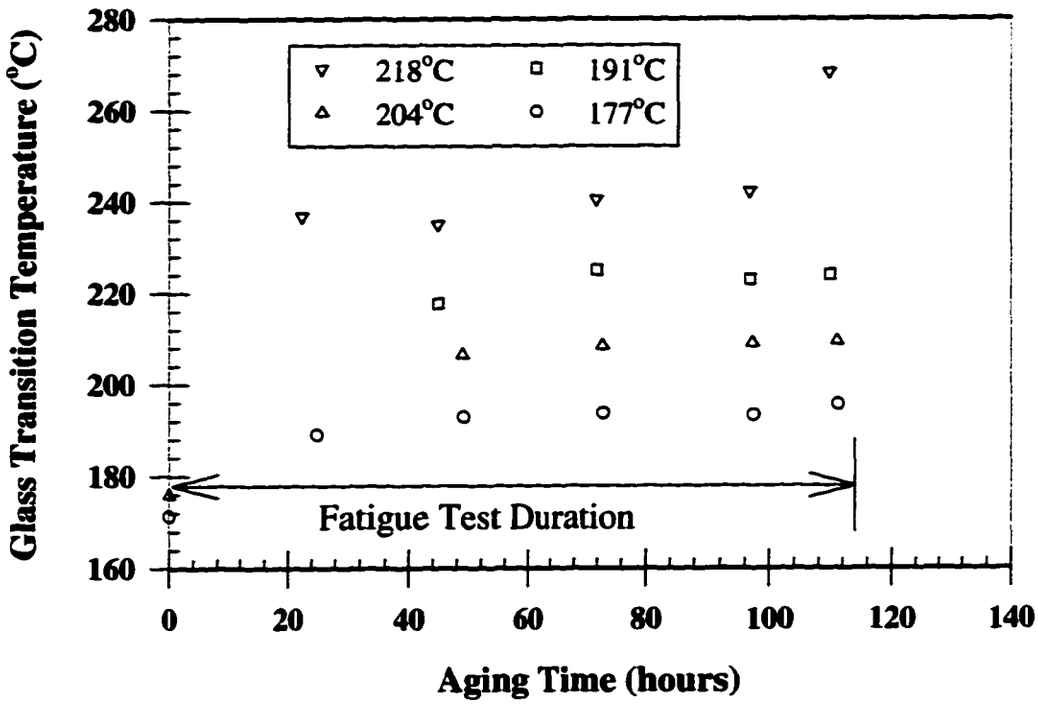

Figure 14. Tg as measured byTMA plotted as a function of aging time.

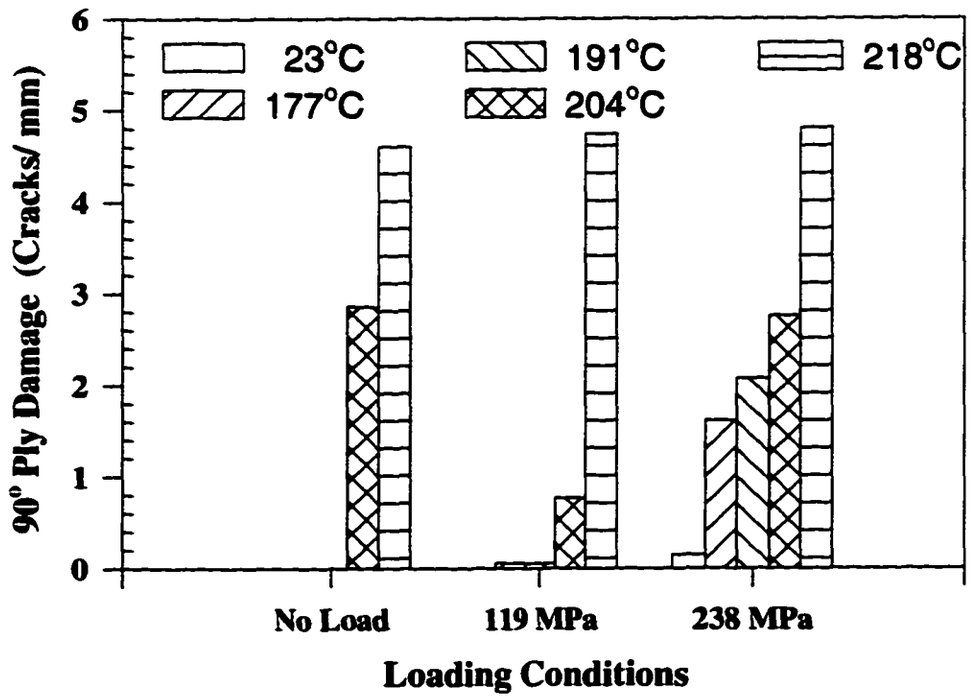

Figure 15. Edge damage in 90^{O} plies for different test temperatures and loading conditions.

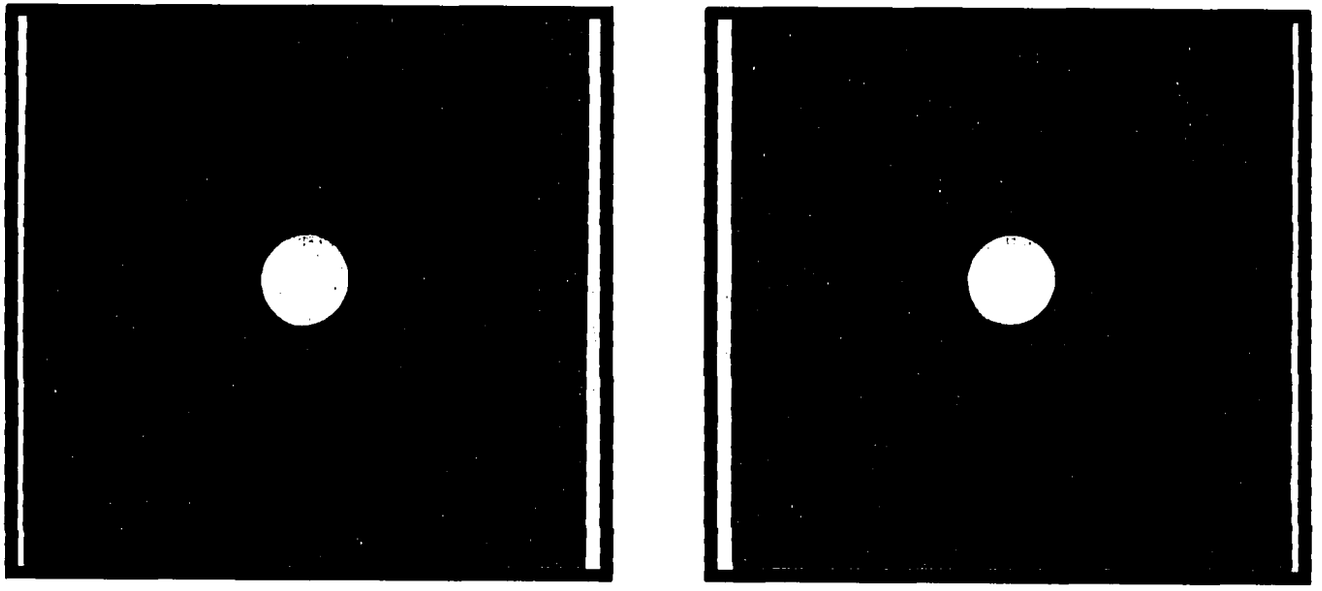

Figure 16. Post fatigue x-ray radiographs of 23°C fatigue tests showing damage accumulation.

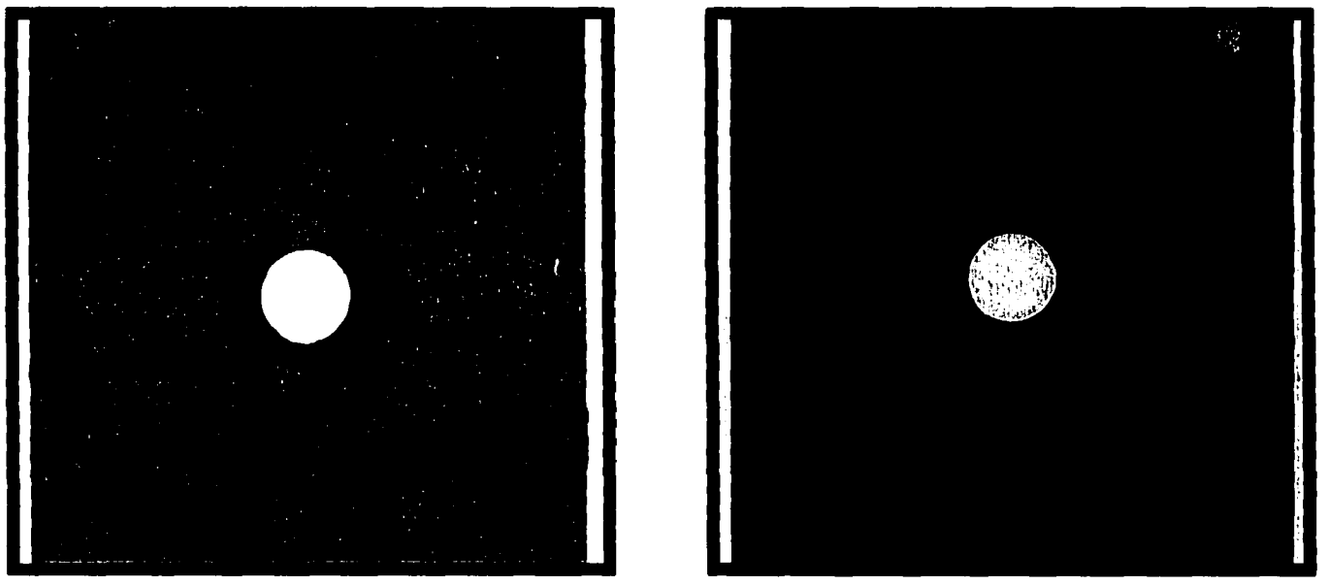

Figure 17. Post fatigue x-ray radiographs of 177°C fatigue tests showing damage accumulation.

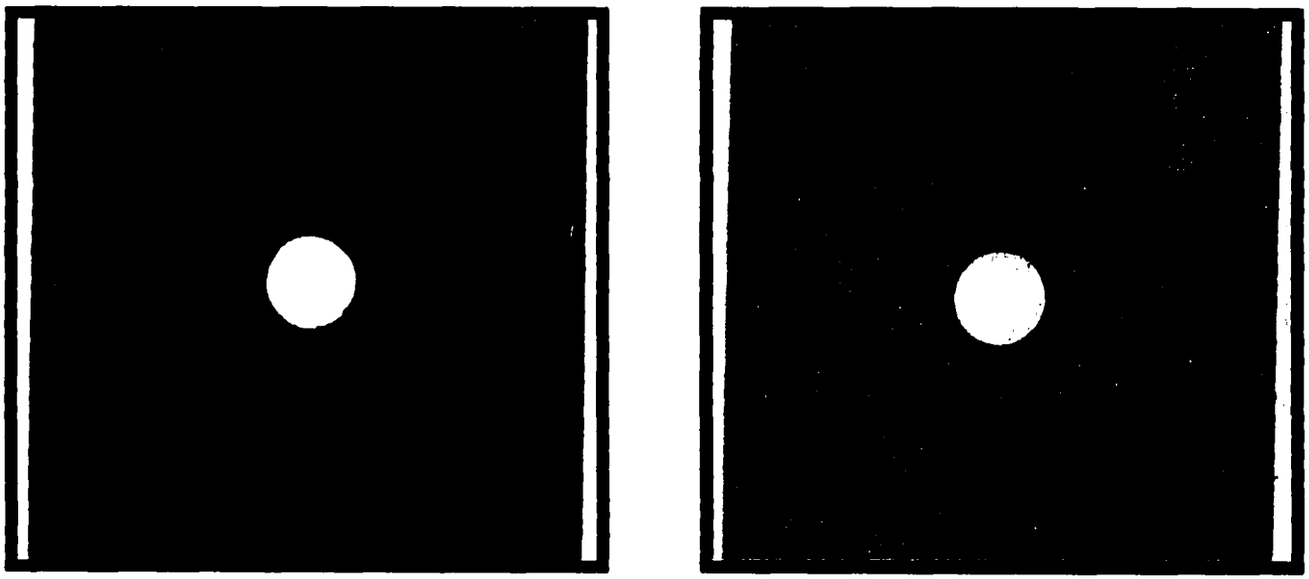

Figure 18. Post fatigue x-ray radiographs of 191°C fatigue tests showing damage accumulation.

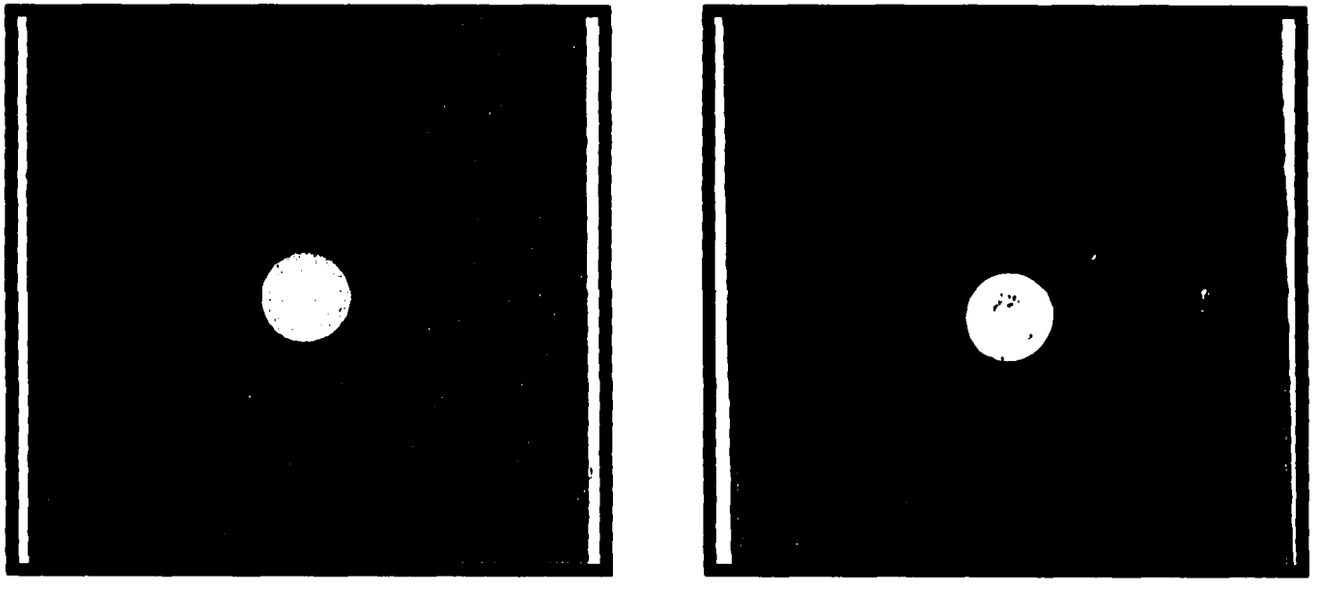

Figure 19. Post fatigue x-ray radiographs of 204°C fatigue tests showing damage accumulation.

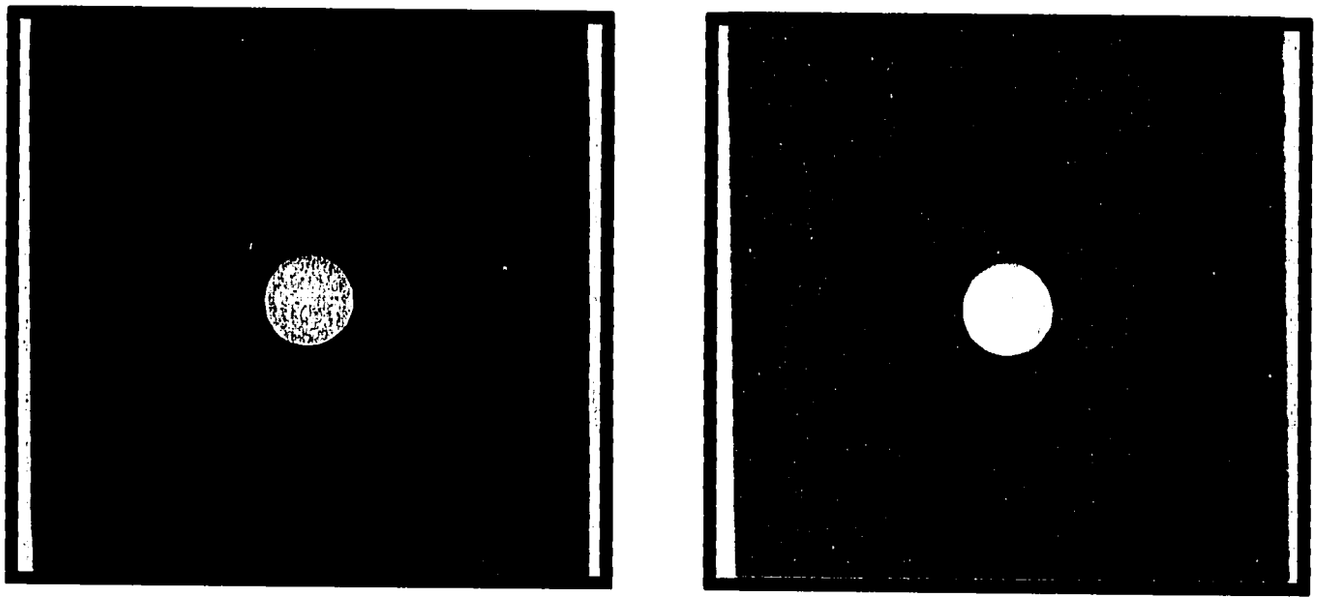

Figure 20. Post fatigue x-ray radiographs of 218°C fatigue tests showing damage accumulation.

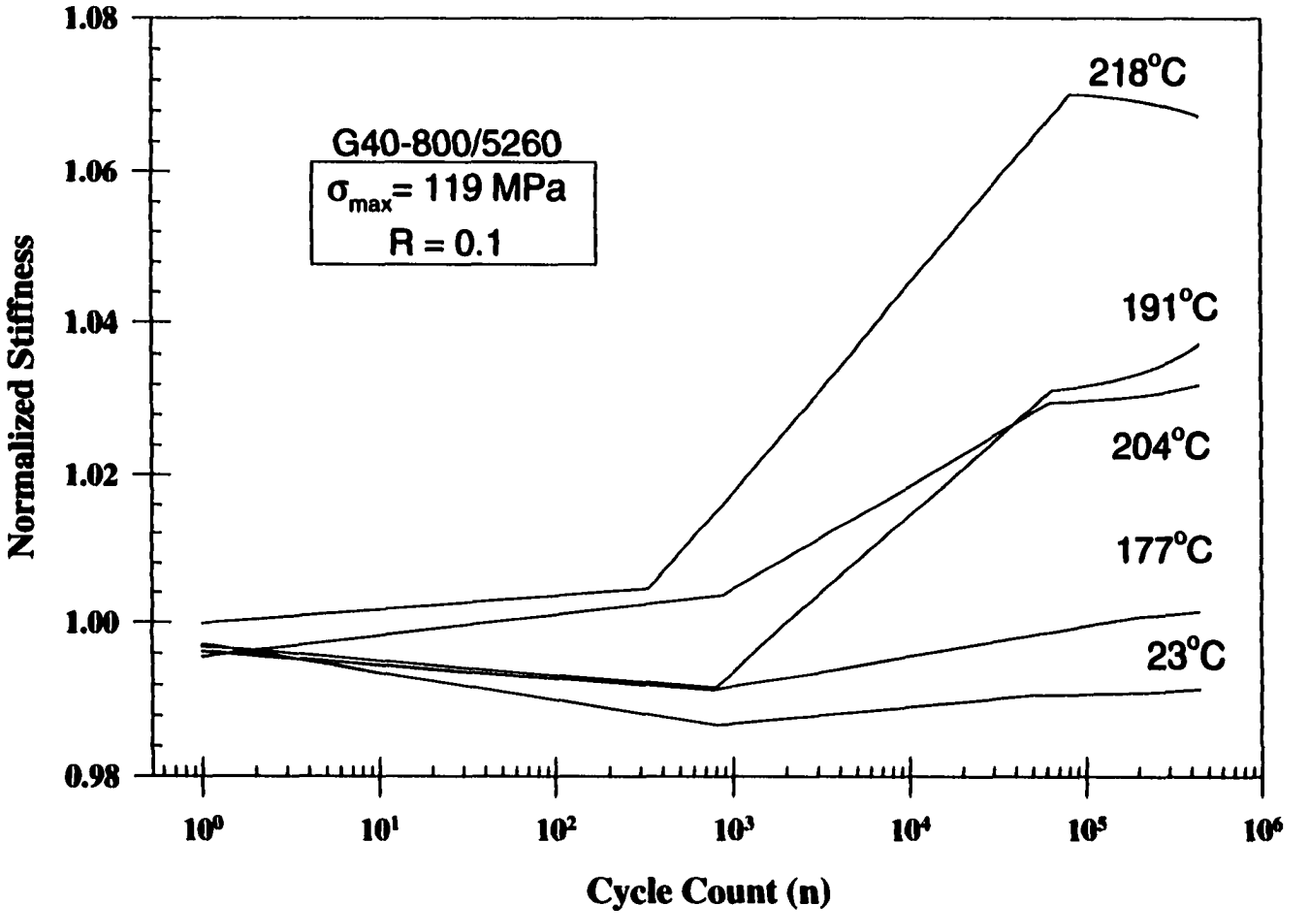

Figure 21. Normalized stiffness of OHT specimens during the low load fatigue tests at each temperature.

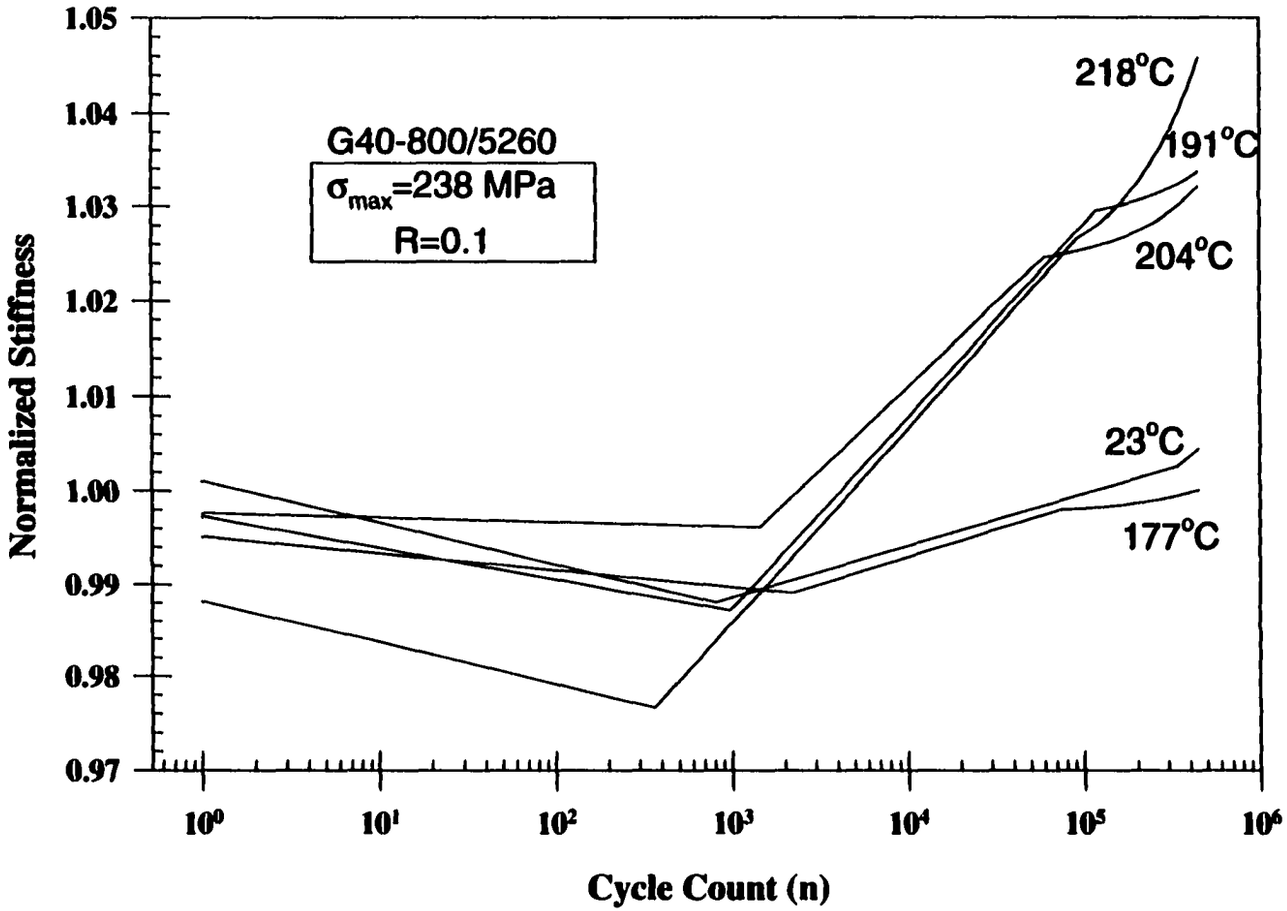

Figure 22. Normalized stiffness of OHT specimens during the high load fatigue tests at each temperature.

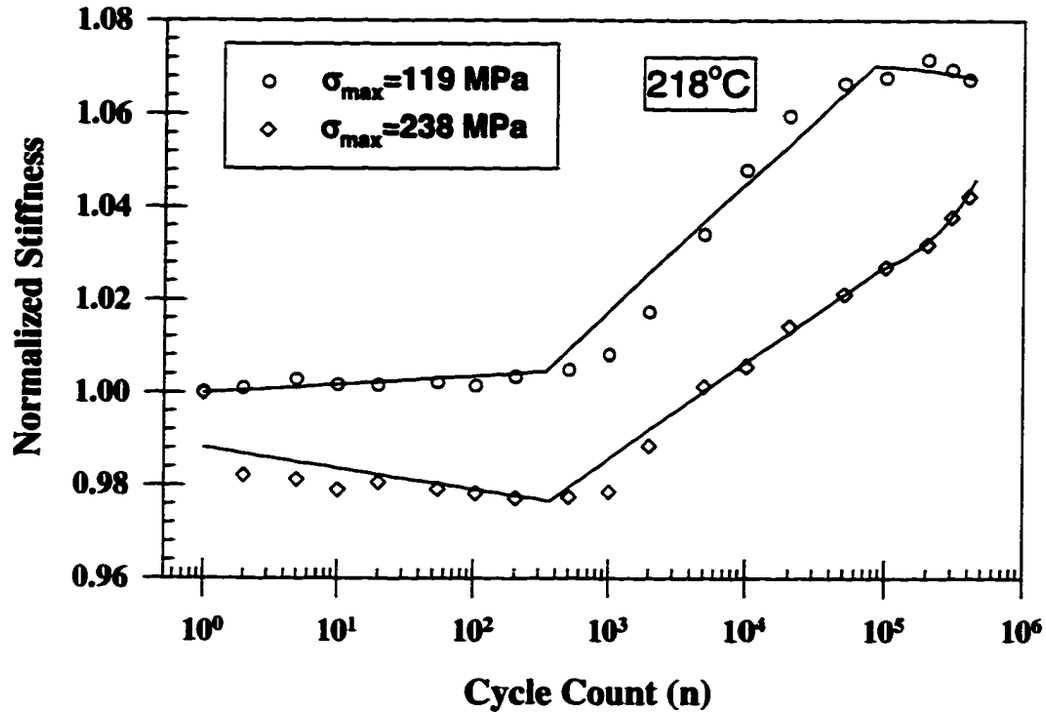

Figure 23. The effect of load level on stiffness results illustrated for the 218°C test temperature.

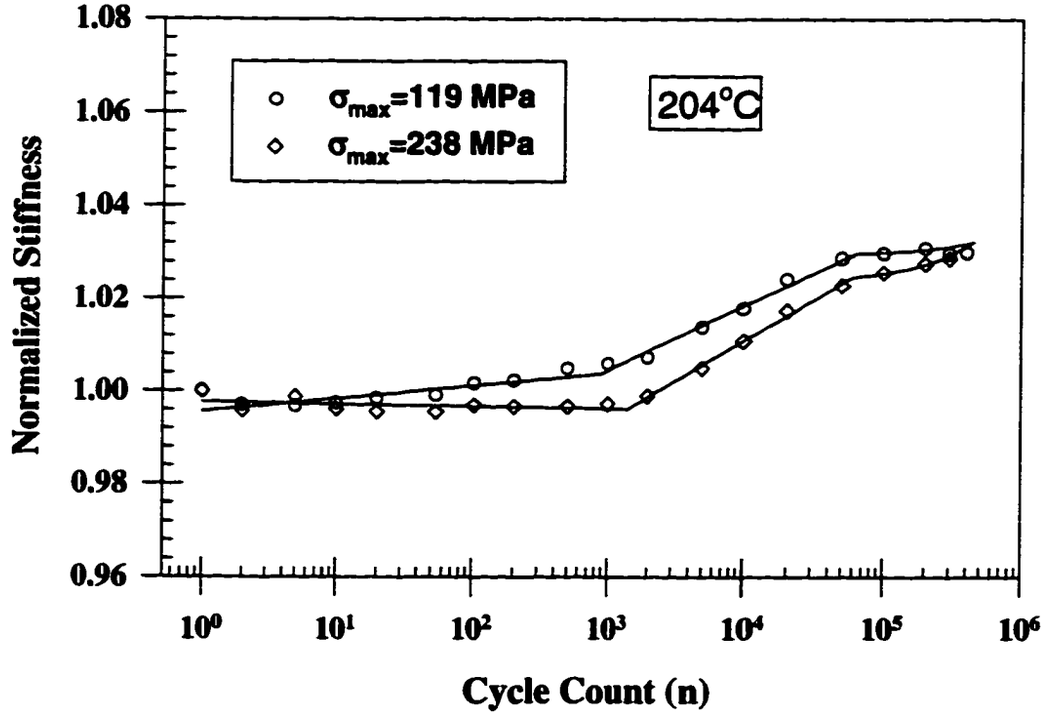

Figure 24. The effect of load level on stiffness results illustrated for the 204°C test temperature.

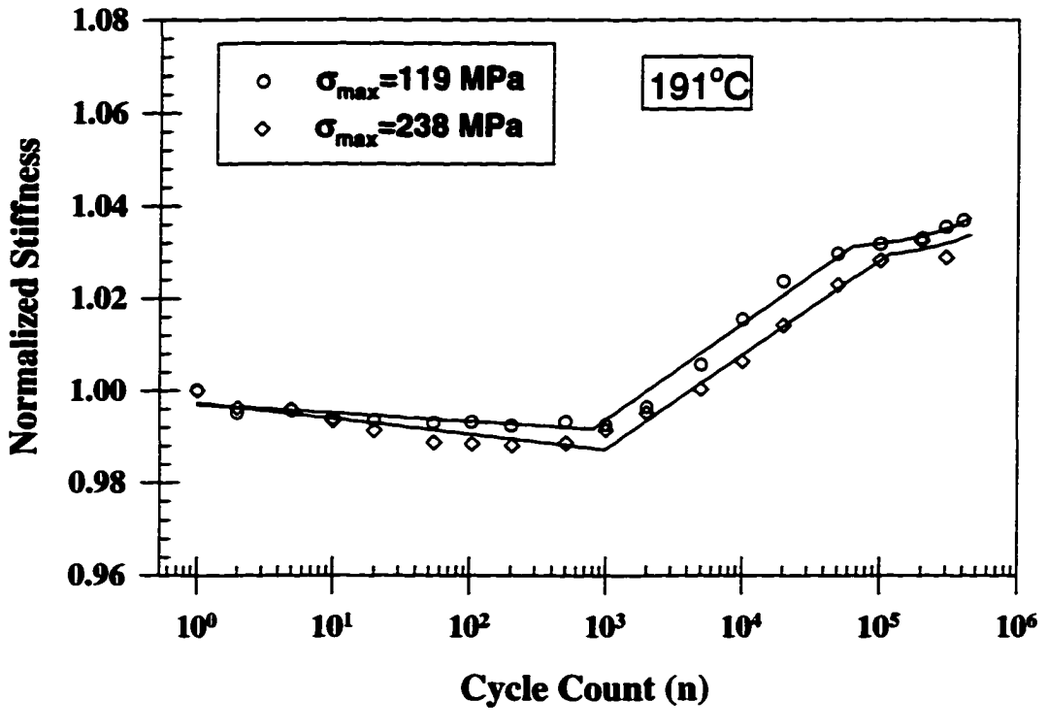

Figure 25. The effect of load level on stiffness results illustrated for the 191°C test temperature.

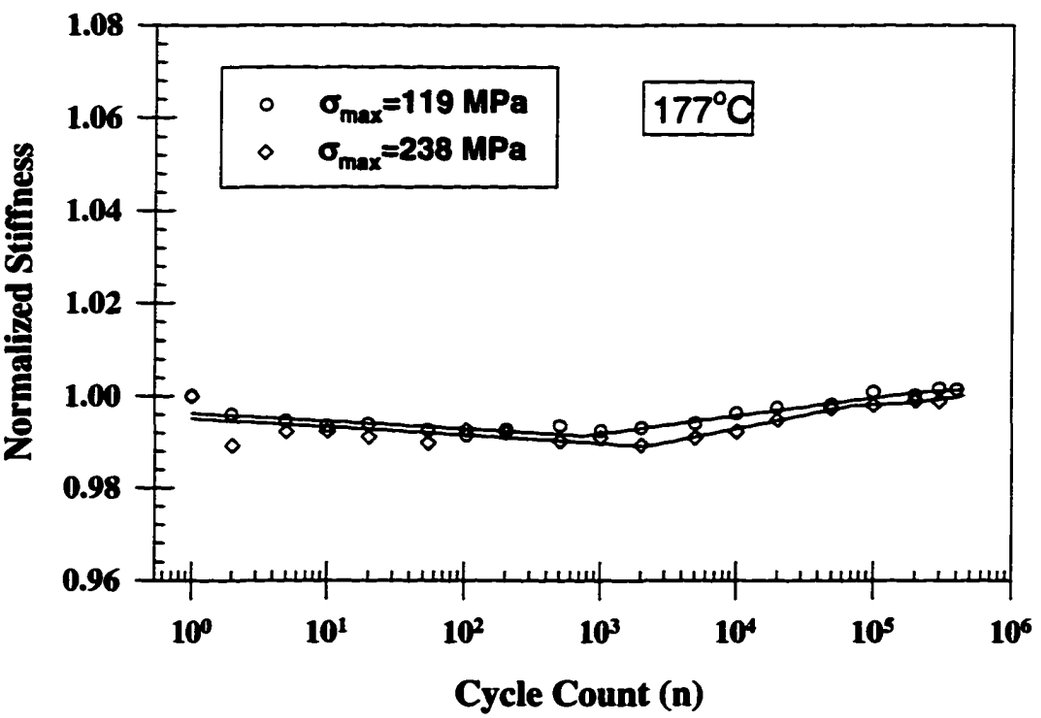

Figure 26. The effect of load level on stiffness results illustrated for the 177°C test temperature.

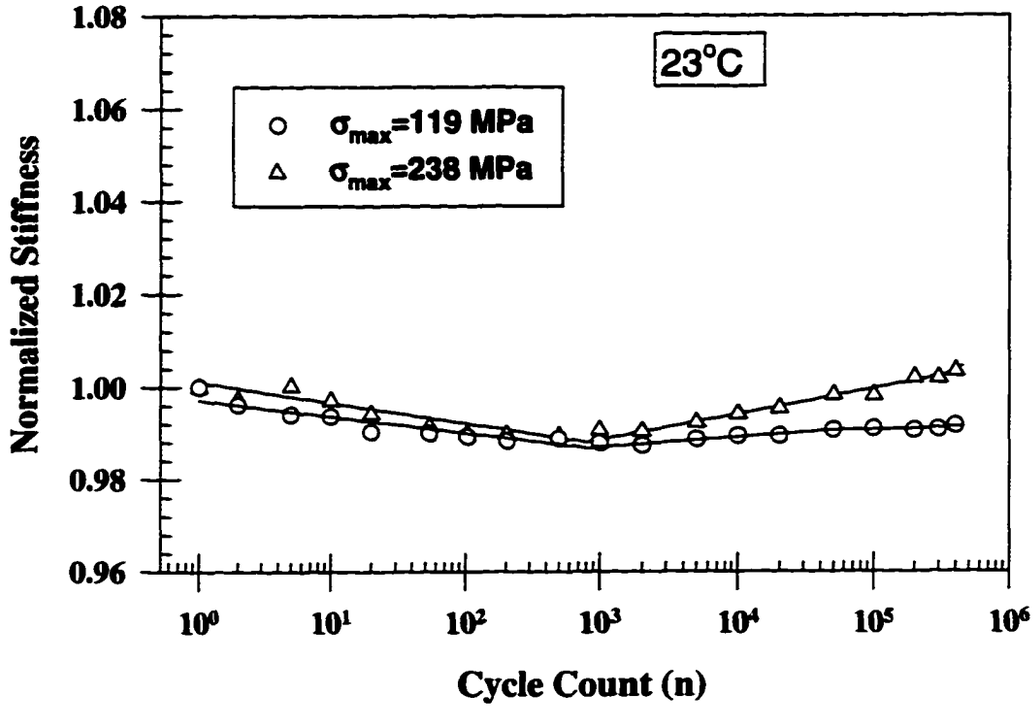

Figure 27. The effect of load level on stiffness results illustrated for the 23°C test temperature.

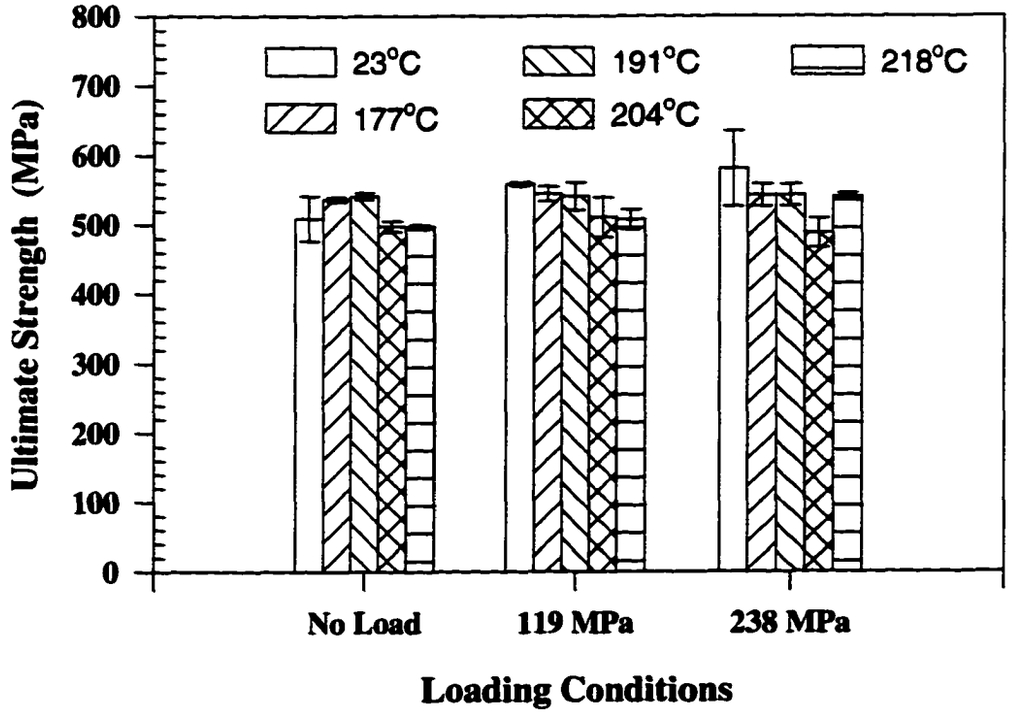

Figure 28. Residual tensile strength of G40-800/5260 OHT specimens after fatiguing or isothermal aging at test temperature.

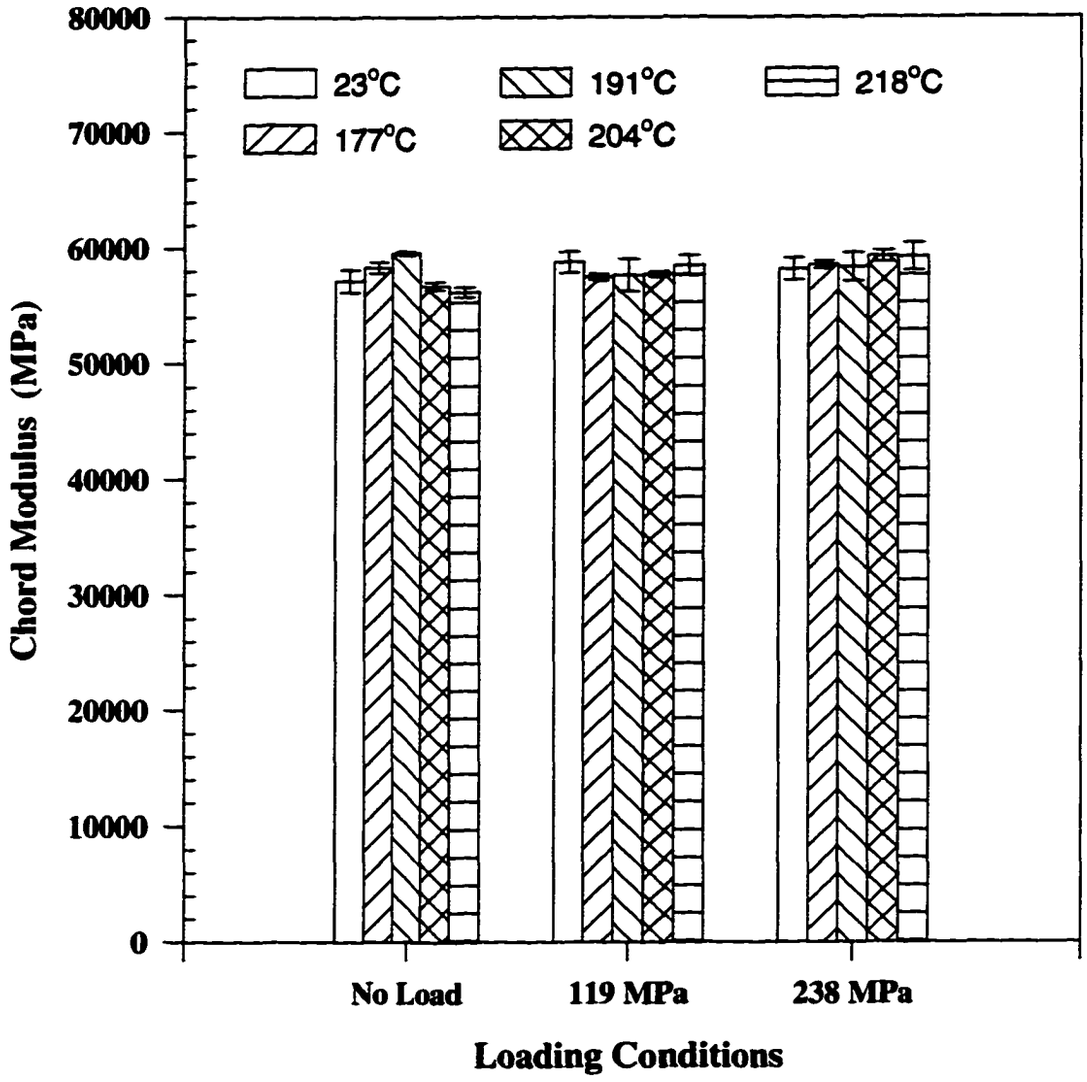

Figure 29. Residual chord modulus of G40-800/5260 OHT specimens after fatiguing or aging at test temperature.

CHAPTER V

SUMMARY AND CONCLUSIONS

Summary

Physical Properties

Chemical aging consisted of two distinct mechanisms that are inter related. Chemical aging includes continuation of the cure and oxidative break down. While the curing effect is present at all of the elevated test temperatures the oxidative breakdown only appears above 191°C. The 177°C and 191°C aging tests experienced an initial weight loss during the first 24 hours which then stabilized. The 204°C and 218°C aging tests showed weight loss that continued to increase during the entire 120 hour aging times. This increasing weight loss trend was most extensive at the highest test temperature. These results demonstrate problems with the materials thermal oxidative stability. Exposure to elevated temperature also caused shifts in T_g which were indicated by both the TMA and DMA data. These shifts indicate that the material continued to cure during aging at all elevated test temperatures.

The changes in the glass transition temperature increase with aging temperature. The 218°C data showed a greater increase in Tg than the 191°C data, and the 204°C data showed a greater increase in Tg than the 177°C data. Since the 191°C and the 204°C data set specimens were exposed to ambient conditions and allowed to absorb moisture, the Tg measured for these temperatures is lower. No direct comparison can be made between the specimens that were exposed to ambient conditions and those that were not since the magnitude of the effect caused by the

moisture absorption is unknown. Although no direct comparison is possible, it was evident that increasing aging temperature increases the effects of aging (indicated by increases in Tg) which is shown by both TMA and DMA data.

Laminate Damage

The level of internal damage was primarily governed by the stress level and not temperature. Radiographs of the higher load showed substantial internal damage at all test temperatures while the low load condition showed minimal damage. At the higher load, where significant levels of damage were present, increasing the test temperature actually decreased the length and number of internal matrix cracks. The decrease of damage as the temperature increased could have been dependent on the behavior of the matrix material. As the temperature is increased, the stiffness of the matrix decreases and so does its tendency to crack. This resulted in the worst internal damage occurring at the high stress, room temperature case.

Increasing the test temperature produced increased levels of edge cracking. The highest amount of edge damage occurred at the highest load level and highest temperature. At the higher temperatures, 204°C and 218°C, extensive matrix cracking was present at all of the loading conditions including the unloaded aging. The edge cracking is deceptive if taken alone to represent extensive internal damage since the high and rather constant level of matrix cracking at the highest temperature could be taken as a point where some characteristic damage state, or matrix crack saturation has occurred [7, 19]. A saturated internal damage state was not demonstrated in the x-ray radiographs. These results demonstrated that for the elevated temperature OHT test,

edge damage alone can not be used as a clear indication of the extent of internal damage.

Chemical aging resulted in the breakdown of the composite as shown by the weight loss data. As stated in the physical properties section, the weight loss demonstrated problems with thermal oxidative stability. This chemical aging damage is a surface phenomena not observable on the x-rays due to its shallow depth of penetration. The high levels of edge damage at 218°C do not represent characteristic damage from the fatigue loading but represent an effect of chemical aging. This explains why the unloaded isothermally aged specimens showed similar levels of damage as the fatigued specimens.

Fatigue Stiffness

The effects of aging on stiffness during fatigue are most clearly demonstrated by the low stress level fatigue results (figure 20), since damage was not a major influence. The low stress level fatigue tests had minimal and equivalent damage for all temperatures tested. The changes in stiffness during fatigue follows trends expected from curing of BMI materials. As the temperature is increased so is the rate of cure and the final extent of cure[11-14]. This was demonstrated in the fatigue stiffness and Tg results since stiffness and Tg are governed by the extent of cure.

As temperature was increased the effects of aging on stiffness increased up to 191°C. This trend is easy to see in the figure of the low stress results (figure 20). This trend seems to change near 191°C and 204°C where the higher rate of stiffness increase occurred with the lower temperature (191°C). The 191°C data and the 204°C data for

the high and low load cases are plotted in figures 30 and 31, respectively. A plausible explanation results from an examination of edge damage. Although edge damage is not a good indicator of internal damage it is a good indicator of thermal oxidative breakdown. At 204°C the unloaded OHT specimens displayed extensive edge cracking while the 191°C specimens aged without load showed no cracks. In addition, at 204°C the specimens displayed continued weight loss throughout while the 191°C specimens did not. These changes, that occur at 204°C, indicate a temperature dependent breakdown of the material that could have influenced the trend of stiffness increase.

The high load stiffness results (figure 22) show the effects of both aging and damage. In contrast to the low load fatigue results, the high stress x-ray data illustrated extensive damage at all temperatures. The effect of damage at elevated temperature is shown in the high load data. When compared to the low load results the high load results show a greater stiffness loss during the first 1000 cycles and stiffness values were generally lower than during the low load results. In addition the high load result have a lower normalized stiffness during the fatigue tests than low lad results.

The complexity that occurs in interpreting stiffness data when the effects of aging and damage are combined are demonstrated by the 177°C data (figure 26). The high load case demonstrated much more damage than the low load case even though the stiffness during their respective fatigue lives are nearly identical. These results show that stiffness is not an effective metric for internal damage when aging effects are present.

Residual Static Properties

Residual strength was taken as the maximum load carrying capability of the laminate during the course of the static test as explained in the procedure section. Examination of the data in figure 28 reveals that the highest strength was associated with the room temperature high load fatigue case while the lowest strength was associated with the high load fatigue and next to highest temperature. The baseline strength values were lower than the strength values for most of the fatigue tests as expected since there was no blunting of the stress concentration due to damage. At room temperature an increase in fatigue load increases damage and results in increased residual strength of the specimen. The high load, room temperature tests showed the highest strength and greatest level of internal damage.

Both high and low stress fatigue data show decreasing strength with an increase in test temperature. The decrease in strength with the increase in temperature for the high fatigue load can be explained since the amount of internal damage decreases with an increase in temperature. As temperature increased, the blunting caused by damage decreased. At the low fatigue load, where minimal damage was present, the strength also decreased with an increase in the temperature during fatigue testing. This observation demonstrates that even when internal damage is minimal or undetectable, aging can affect the specimens strength.

Small changes in residual static stiffness were observed during monotonic tests of the previously fatigued specimens, as shown in figure 29. The highest stiffness was associated with the 191°C, unloaded specimens while the lowest stiffness was

associated with the unloaded baseline specimens at the highest aging temperature. The trends that are apparent in fatigue stiffness data are not apparent in the static stiffness data. This is because the static modulus results are based on only two tests, so the specimen to specimen could hide trends of a small magnitude. Since the fatigue test were performed on specimens from many different panels, unlike the unloaded aging study, small variations in static stiffness are expected. In addition, the placement and alignment of the extensometer could add to the uncertainty of each test. Because the fatigue data was normalization, many of these problems of alignment and specimen variation were not present in the fatigue results.

Conclusions

The objective of this research was to determine the effects of elevated temperature and fatigue loading on a graphite/bismaleimide composite. These responses were then related to physical processes known to cause changes in the mechanical performance of PMCs. Two processes that change the mechanical performance during elevated temperature fatigue were evident. These mechanisms were aging and fatigue damage accumulation.

The chemical aging consisted of two individual parts; continuation of cure and oxidative breakdown. The presence of chemical aging was shown by the physical properties tests. The continuation of cure was demonstrated by the shifts in Tg. The measured increases in glass transition temperature of the G40-800/5260 material demonstrated that over time the elevated test temperature advances the extent of cure in the matrix. The TMA and DMA data also established that higher test temperatures

caused greater curing effects. Extended exposure to extreme environments also caused thermal oxidative breakdown. This was illustrated by continued weight loss over time and the presence of aging induced edge damage on the unloaded and fatigued OHT specimens.

Open hole tension fatigue tests of the composite at elevated temperatures produced stiffness changes in the gage section of the laminate which were dependent upon the relative contributions of damage development and aging. During the fatigue tests, aging of the polymer in the laminate induced a time and temperature dependent increase in stiffness which competed with decreases in stiffness due to load-dependent damage. The higher the temperature the higher the rate and level of stiffness gain. This phenomenon followed the curing trends in the physical property data.

The residual static properties were demonstrate effects caused by both aging and fatigue damage. Aging changed the residual strength of the composite laminate when damage was minimal or nonexistent. Increases in OHT static strength occurred with the increase in damage around the notch.

Edge damage was shown to be a poor indicator the extent of internal damage since the edge damage measurements included effects of chemical aging with the effects of internal damage. At elevated temperature the stiffness was also a poor indicator of internal damage. The stiffness gained during aging prevented isolation of the effects of damage during stiffness measurements.

Increases in Tg, continued weight loss, temperature dependent stiffness changes, damage dependent stiffness change, and possibly loading dependent stiffness

change all affected the mechanical performance. These factors demonstrate that the processes of aging and damage accumulation should not be considered separately in determining mechanical properties during high temperature testing since they are interdependent. Time and temperature dependent interactions are sometimes ignored for the sake of economical feasibility of testing but should be considered for accuracy.

It is apparent that use of the OHT test to characterize the elevated temperature fatigue performance of G40-800/5260 requires knowledge of the relative contributions of aging and damage to the fatigue and post-fatigue behavior. Synergistic contributions of effects caused by these processes may result in a net laminate stiffness increase for a given temperature and stress level. Properly modeling of the long term behavior of materials subjected to use where aging and damage accumulation play critical roles requires an understanding of the interactions of these processes.

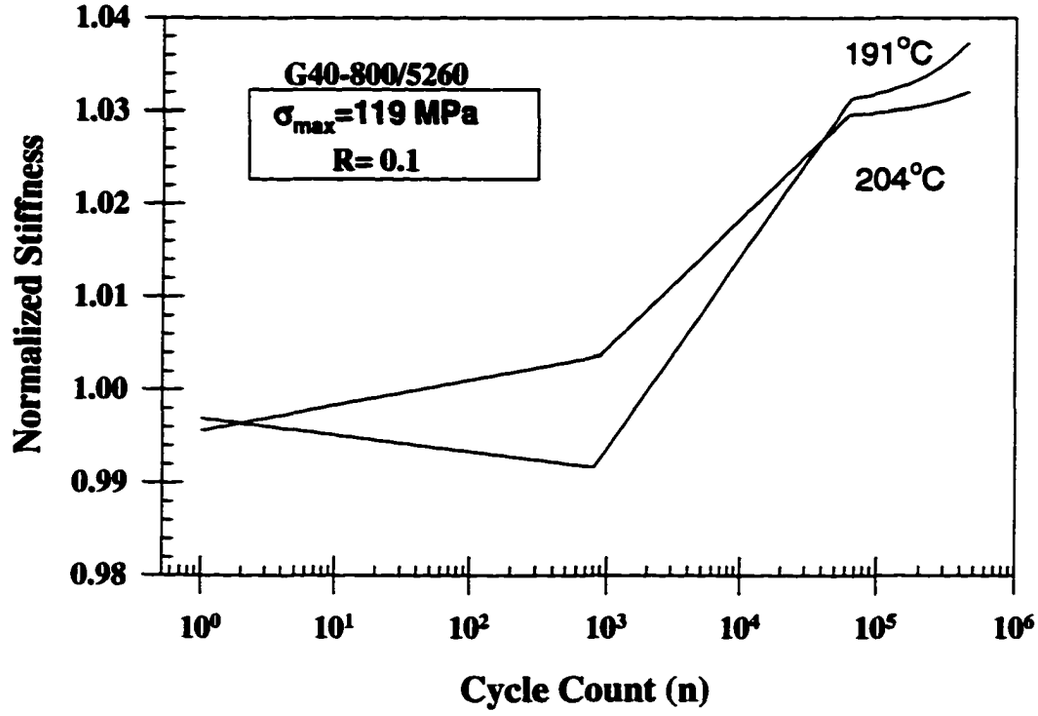

Figure 30. Detail of normalized stiffness of OHT specimens during the low load fatigue tests at 191°C and 204°C.

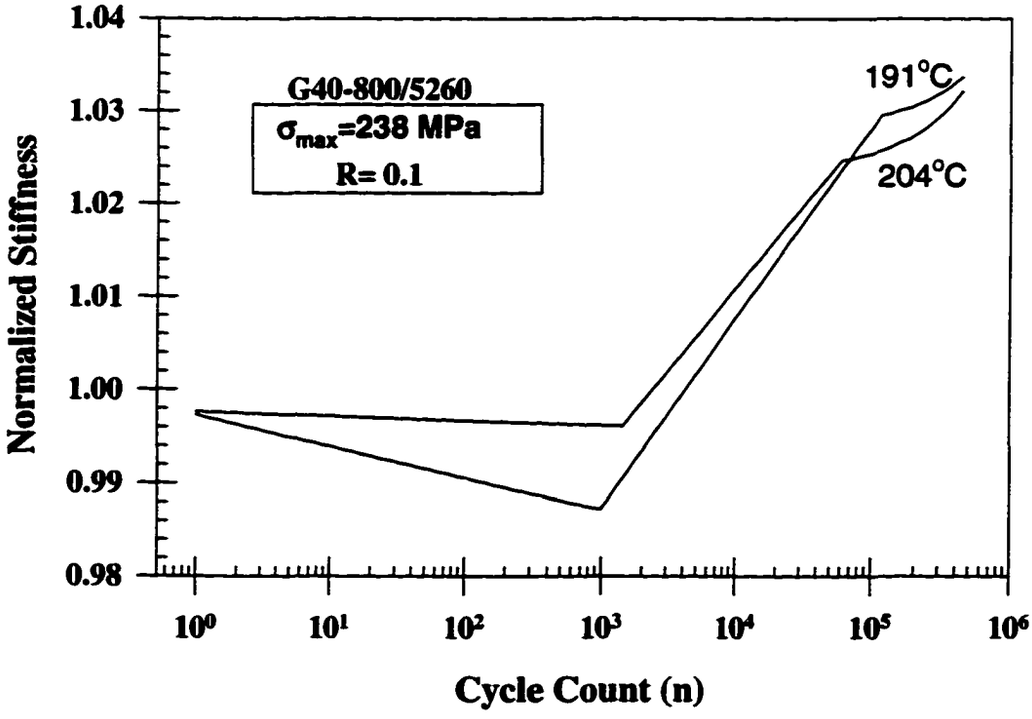

Figure 31. Detail of normalized stiffness of OHT specimens during the high load fatigue tests at 191°C and 204°C.

REFERENCES

[1] Coats, T. W., and Harris, C. E., "Experimental Verification of a Progressive Damage Model for IM7/5260 Laminates Subjected to Tension-Tension Fatigue," *Journal of Composite Materials*, Vol. 29, 1995, pp. 280-305.

[2] Allen, D. H., Harris, C. E., and Groves, S. S., "A Thermomechanical Constitutive Theory for Elastic Composites with Distributed Damage- I. Theoretical Development," *International Journal of Solids and Structures*, Vol. 23, No. 9, 1987, pp. 1301-1318.

[3] Allen, D. H., Harris, C. E., and Groves, S. S., "A Thermomechanical Constitutive Theory for Elastic Composites with Distributed Damage- II. Application to Matrix Cracking in Laminated Composites," *International Journal of Solids and Structures*, Vol. 23, No. 9, 1987, pp. 1319-1338.

[4] Harris, C. E., and Allen D. H., "A Continuum Damage Model of Fatigue-Induced Damage in Laminated Composites," *SAMPE Journal*, July/August, 1988, pp.43-51.

[5] Lee, J. W., Allen D. H., and Harris C. E. "Internal State Variable Approach for Predicting Stiffness Reduction in Fibrous Laminated Composites with Matrix Cracks," *Journal of Composite Materials*, Vol. 23, December, 1989, pp.1273-1277.

[6] Talreja, R., "A Continuum Mechanics Characterization of Damage in Composite Materials," *Proceedings of the Royal Society of London, A*, Vol. 399, 1985, pp. 195-216.

[7] Talreja, R., *Fatigue of Composite Materials*, Lancaster Pennsylvania, Technomic Publishing Company, Inc., 1987.

[8] Struik, L. C. E., *Physical Aging in Amorphous Polymers and Other Materials*. New York: Elsevier Scientific Publishing Company, 1978.

[9] Wang, X., and. Gillham, J. K, "Physical Aging in the Glassy State of a Thermosetting System vs. Extent of Cure," *Journal of Applied Polymer Science*, Vol. 47, 1993, pp. 447-460.

[10] Zhou, J., "A Constitutive Model of Polymer Materials Including Chemical Aging and Mechanical Damage and its Experimental Verification," *Polymer*, Vol. 34, 1993,. pp. 4252-4256

[11] White, S. R., and Hahn, H. T., "Mechanical Properties and Residual Stress Development During Cure of a Graphite/BMI Composite", *Polymer Engineering and Science*, Vol. 30, No. 22, 1990, pp. 1465-1473.

[12] White, S. R., and Hahn, H. T., "Process Modeling of Composite Materials: Residual Stress Development During Cure. Part I. Model Formulation", *Journal of Composite Materials*, Vol. 26, No. 16, 1992, pp. 2402-2421.

[13] White, S. R., and Hahn, H. T., "Process modeling of Composite Materials: Residual Stress Development During Cure. Part II. Experimental Validation", *Journal of Composite Materials*, Vol. 26, No. 16, 1992, pp. 2423-2453.

[14] White, S. R., and Hahn, H. T., "Cure Cycle Optimization for the Reduction of Processing-Induced Residual Stresses in Composite Materials", Journal of Composite Materials, Vol. 27, No. 14, 1993, pp. 2402-2421.

[15] Browning, C. E., and Schwartz, H. S. "Delamination Resistant Composite Concepts," *Composite Materials: Testing and Design (Seventh Conference)*, ASTM STP 893, J. M. Whitney, Ed., American Society for Testing and Materials, Philadelphia, 1986, pp. 256-265.

[16] Masters, J. E., "Characterization of Impact Damage Development in Graphite/Epoxy Laminates," *Fractography of Modern Engineering Materials: Composites and Metals*, ASTM STP 948, J. E. Masters and J. J. Au, Eds., American Society for Testing and Materials, Philadelphia, 1987, pp. 238-258.

[17] Altus, E., and Ishai, O, "The Effect of Soft Interleaved Layers on the Transverse Cracking/Delamination Mechanisms in Composite Laminates," *Composites Science and Technology*, Vol. 39, 1990, pp. 13-27.

[18] Bakis, C. E. and Stinchcomb, W. W., "Response of Thick, Notched Laminates Subjected to Tension-Compression Cyclic Loads," *Composite Materials: Fatigue and Fracture*, ASTM STP 907, H. T. Hahn, Ed., American Society for Testing and Materials, Philadelphia, 1986, pp. 314-334.

[19] Riefsnider, K. L., Schulte, K., and Duke. J. C., "Long-Term Fatigue Behavior of Composite Materials," *Long-Term Behavior of Composites*, ASTM STP 813, T. K. O'Brien, Ed., American Society for Testing and Materials, Philadelphia, 1983, pp. 136-159.

[20] Baron, Ch., and Schulte, K., *Fatigue Damage Response of CFRP with Toughened Matrixes and Improved Fibres*, pp. 4.65-4.75.

[21] Kellas, S., Morton, J., and Bishop S. M., "Fatigue Damage Development in a Notched Carbon Fiber Composite," *Composite Structures*, Vol. 5, 1986, pp.143-157.

[22] Baron, Ch., Schulte, K., and Harig, H., "Influence of Fiber and Matrix Failure Strain on Static and Fatigue Properties of Carbon Fiber-Reinforced Plastics," *Composites Science and Technology*, Vol. 29, 1987, pp. 257-272.

[23] Scrivner, G. C. and Chan, W.S., "Effects of Stress Ratio on Edge Delamination Characteristics in Laminated Composites," *Composite Materials: Fatigue and Fracture*, Fouth Volume, ASTM STP 1156, W. W. Stinchcomb and N. E. Ashbaugh, Eds., American Society for Testing and Materials, Philadelphia, 1993, pp. 538-551.

[24] Henaff-Gardin, C., and Lafarie-Frenot, M. C., "Fatigue Behavior of Thermoset and Thermoplastic Cross-Ply Laminates," *Composites*, Vol. 23, No. 2, March 1992, pp.109-116.

[25] Prinz, R., "CRP Damage Mechanics, A Survey," Lecture delivered at Structural Mechanics Conference of July 2, 1987, European Space Agency-Technical Translation, ESA-TT-1093, September 1988, pp. 8-30.

[26] Chu, G. D., and Sun, C. T., "Failure Initiation and Ultimate Strength of Composite Laminates Containing a Center Hole," *Composite Materials: Fatigue and Fracture*, Fourth Volume, ASTM STP 1156, W. W. Stinchcomb and N. E. Ashbaugh, Eds., American Society for Testing and Materials, Philadelphia, 1993, pp. 35-54.

[27] Wolterman, R. L., Kinnidy, J. M., and Farley, G. L, "Fatigue Damage in Thick Cross-Ply Laminates with a Center Hole," *Composite Materials: Fatigue and Fracture*, Fourth Volume, ASTM STP 1156, W. W. Stinchcomb and N. E. Ashbaugh, Eds., American Society for Testing and Materials, Philadelphia, 1993, pp. 473-490.

[28] Lo, K. H., Wu, E. M., and Konishi, D. Y., "Failure Strength of Notched Composite Laminates," *Journal of Composite Materials*, Vol. 17, September 1983, pp. 384-397.

[29] Swain, R. E., Bakis, C. E, and Reifsnider, K. L., "Effect of Interleaves on the Damage Mechanisms and Residual Strength of Notched Composite Laminates Subjected to Axial Fatigue Loading" *Composite Materials: Fatigue and Fracture*, Fourth Volume, ASTM STP 1156, W. W. Stinchcomb and N. E. Ashbaugh, Eds., American Society for Testing and Materials, Philadelphia, 1993, pp. 552-574.

[30] Kirschke, L., "Investigations Into Initiation and Propagation of Damage in Notched Uni- and Multi-directional CRP Laminates" Lecture delivered at Structural Mechanics Conference of July 2, 1987, European Space Agency-Technical Translation, ESA-TT-1093, September 1988, pp. 70-93.

[31] Kerr, J. R., Haskins, J. F., "Time-Temperature-Stress Capabilities of Composite Materials for Advanced Supersonic Technology Application", NASA Contractor Report 178272, May 1987.

[32] Martin, R. H., 1991, "Delamination Onset in Polymeric Composite Laminates Under Thermal and Mechanical Loads," NASA Contractor Report-189548, November 1981.

[33] Chan, W. S., Rogers, C., and Aker, S., "Improvement of Edge Delamination Strength of Composite Laminates Using Adhesive Layers," *Composite Materials: Testing and Design*, Seventh Conference, ASTM STP 893, J. M. Whitney, Ed., American Society for Testing and Materials, Philadelphia, 1986, pp. 266-285.

[34] Kim, R. Y., and Crasto, A. S., 1995, "Measurement of Residual Strains in Composite Laminates by Ply Separation", Proceedings of the 1995 SEM Spring Conference and Exhibit, June 12-14, 1995, Grand Rapids, Michigan, Society for Experimental Mechanics, pp. 533-540.

[35] McManus, H., L., Bowles, D. E., and Tomkins, S. S., 1996, "Prediction of Thermal Cycling Induced Matrix Cracking", *Journal of Reinforced Plastics and Composites*, Vol. 15, pp. 124-140.

[36] Kenny, J. M., Trivisano, Al, and Nicolais, L., 1993, "Thermal Characterization of the Cure Kinetics of Advanced Matrices for High-performance Composites", *Advances in Chemistry Series-Toughed Plastics I*, Riew, C. K., and Kinloch, A. J., Editors., American Chemical Society, Washington, D. C. pp. 539-557.

[37] Salin, I. M., Seferis, J. C., Loechelt, C. L., and Rothschilds, R., 1992, "Time-Temperature Equivalence in Thermogravimetery for BMI Composites", *SAMPE Quarterly*, Vol. 24, No. 1, pp. 54-63.

[38] Nam, J. D, and Seferis, J. C. 1992, "Anisotropic Thermo-Oxidative Stability of Carbon Fiber Reinforced Polymeric Composites", *SAMPE Quarterly*, Vol. 24, No. 1, pp. 10-18.

[39] Hinkley, J. A., and Yue, J. J., "Oxidative Aging of Thermoplastic Polyimide Films", *Journal of Applied Polymer Science*, Vol. 57, 1995, pp. 1539-1543.

[40] Hirschbuehler, K. R., "An Improved 270F Performance Interleaf System Having Extremely High Impact Resistance," *SAMPE Quarterly*, Vol. 17, No. 1, October 1985, pp. 46-49.

[41] Boyd, J. D., and Chang, G., " A Third-Generation Bismaleimide Prepreg System," 35th International SAMPE Symposium, April 2-5, 1990, Vol.35, Book 1 of 2, pp. 994-1006.

[42] Martin, R. H., Siochi E. J., and Gates T. S., "Isothermal Aging of IM7/8320 and IM7/5260," NASA Technical Memorandum 107666, August 1992.

[43] Tuttle, M. E., Delaney, A., and Emery, A. F., 1995, "Mass Loss and residual Stiffness and Strength of IM7/5260 Composites Subjected to Elevated Loads and Temperature", Proceedings of the 1995 SEM Spring Conference and Exhibit, June 12-14, 1995, Grand Rapids, Michigan, Society for Experimental Mechanics, pp. 499-506.

[44]Yang, Q., and Engblom, J. J., "Finite Element Based Sub-Laminate Damage Model For Intraply Cracking," *Journal of Reinforced Plastics and Composites*, Vol.14, March 1995, pp.233-254.

[45]Varna, J., and Berglund, L., "Multiple Transverse Cracking and Stiffness Reduction in Cross-Ply Laminates," Journal of Composites Technology & Research, JCTRER, Vol. 13, No. 2, Summer 1991, pp.99-106.

[46] Bank, L. C., Gentry, T. R., and Barkatt, A., "Accelerated Test Methods to Determine the Long-Term Behavior of FRP Composite Structures: Environmental Effects," *Journal of Reinforced Plastics and Composites*, Vol. 14, pp. 559-587, June 1995.

[47] Whitney, J. M., Daniel, I. M., and Pipes, R. B., *Experimental Mechanics of Fiber Reinforced Composite Materials*, SESA Monograph No. 4, The Society for Experimental Stress Analysis Brookfield Center, Connecticut, 1982.

[48] Browning, C. E., and Schwartz, H. S. "Delamination Resistant Composite Concepts," *Composite Materials: Testing and Design*, Seventh Conference, ASTM STP 893, J. M. Whitney, Ed., American Society for Testing and Materials, Philadelphia, 1986, pp. 256-265.

VITA

WILLIAM M. JOHNSTON

109 LESLIE LANE • YORKTOWN, VIRGINIA • 23693
(W) (757) 865-7093 (H) (757) 867-9069

EDUCATION

1993 - 1997 Old Dominion University — Norfolk, Virginia
Masters of Science in Engineering Mechanics — GPA 3.50

1988 - 1993 Old Dominion University — Norfolk, Virginia
Bachelor of Science in Mechanical Engineering — GPA 3.16

WORK EXPERIENCE

1993 - 1996 Old Dominion Research Foundation — Norfolk, Virginia
Graduate Research Assistant

- Conducted elevated temperature fatigue research on notched polymeric composites at the Mechanics of Materials Branch, NASA Langley Research Center.
  - Analyzed effects damage and chemical aging on the mechanical properties of Graphite/Bismaleimide composite.
  - Developed elevated temperature test methods for composite materials.
  - Designed an experimental set up that allowed in situ, visual microscopic inspection during elevated temperature testing.

1991 - 1992 Old Dominion Research Foundation — Norfolk, Virginia
Undergraduate Research Assistant

- Operated low speed wind tunnel.
- Teaching assistant for a computer aided design lab.

1997 - Analytical Services & Materials, Inc. — Hampton, Virginia
Research Scientist

- Performed fracture testing on aluminum.